OFFICE OF NAVAL RESEARCH

Contract N00014-87-K-0494

R&T Code 400X027YIP

Technical Report No. 7

Nonlocal Free Energy Density Functional Theory Applied to The Electrical Double Layer. I. Symmetrical Electrolytes

by

Zixiang Tang, L. Mier-y-Teran, H.T. Davis, L.E. Scriven, and H.S. White

Prepared for Publication in

Molecular Physics

University of Minnesota
Department of Chemical Engineering and Materials Science
Minneapolis, MN 55455

April 10, 1990

SECURITY CLASSIFICATION OF THIS PAGE

REPORT DOCUMENTATION PAGE

1a. REPORT SECURITY CLASSIFICATION **Unclassified**	1b. RESTRICTIVE MARKINGS
2a. SECURITY CLASSIFICATION AUTHORITY	3. DISTRIBUTION/AVAILABILITY OF REPORT
2b. DECLASSIFICATION/DOWNGRADING SCHEDULE	**Unclassified/Unlimited**
4. PERFORMING ORGANIZATION REPORT NUMBER(S) **ONR Technical Report 7**	5. MONITORING ORGANIZATION REPORT NUMBER(S)
6a. NAME OF PERFORMING ORGANIZATION **Dept of Chemical Engineering and Materials Science** 6b. OFFICE SYMBOL (If applicable) **Code 1113**	7a. NAME OF MONITORING ORGANIZATION **Office of Naval Research**
6c. ADDRESS (City, State, and ZIP Code) **University of Minnesota Minneapolis, MN 55455**	7b. ADDRESS (City, State, and ZIP Code) **800 North Quincy Street Arlington, VA 22217**
8a. NAME OF FUNDING/SPONSORING ORGANIZATION **Office of Naval Research** 8b. OFFICE SYMBOL (If applicable)	9. PROCUREMENT INSTRUMENT IDENTIFICATION NUMBER **Contract No. N00014-87-K-0494**
8c. ADDRESS (City, State, and ZIP Code) **800 North Quincy Street Arlington, VA 22217-5000**	10. SOURCE OF FUNDING NUMBERS PROGRAM ELEMENT NO. / PROJECT NO. / TASK NO. / WORK UNIT ACCESSION NO

11. TITLE (Include Security Classification)

Nonlocal Free Energy Density Functional Theory Applied to The Electrical Double Layer. I. Symmetrical Electrolytes

12. PERSONAL AUTHOR(S)

Zixiang Tang, L. Mier-y-Teran, H.T. Davis, L.E. Scriven and H.S. White

13a. TYPE OF REPORT	13b. TIME COVERED	14. DATE OF REPORT (Year, Month, Day)	15. PAGE COUNT
Technical	FROM 4/10/89 TO 4/10/90	April 10, 1990	24

16. SUPPLEMENTARY NOTATION

submitted to Molecular Physics, January 1990

17. COSATI CODES			18. SUBJECT TERMS (Continue on reverse if necessary and identify by block number)
FIELD	GROUP	SUB-GROUP	

19. ABSTRACT (Continue on reverse if necessary and identify by block number)

A theoretical study of the restricted primitive model of the electrical double layer using a free energy density functional theory is presented. The ion-ion hard-core repulsive contribution to the free energy is incorporated by a nonlocal excess hard-sphere free energy density functional. The electrostatic part of the ion-ion direct correlation function of the inhomogeneous electrolyte in the interfacial region is approximated by that of the homogeneous bulk electrolyte. The generalized van der Waals model and the Tarazona model are used to construct the respective excess hard-sphere free energy density functionals and compared with each other. Each model requires as input a hard equation of state. The Carnahan-Starling equation of state is chosen. The theory predicts correctly the layering effect of the counterions and the charge inversion phenomenon. The results for 1:1 and 2:2 electrolytes agree well with the Monte Carlo simulations. The Tarazona model gives results in closer agreement with Monte Carlo data than does the generalized van der Waals model. The diffuse layer potentials predicted by the Tarazona model are (continued)

20. DISTRIBUTION/AVAILABILITY OF ABSTRACT	21. ABSTRACT SECURITY CLASSIFICATION
☒ UNCLASSIFIED/UNLIMITED ☐ SAME AS RPT ☐ DTIC USERS	**Unclassified**
22a. NAME OF RESPONSIBLE INDIVIDUAL **Henry S. White**	22b. TELEPHONE (Include Area Code) **(612) 625-6995** 22c. OFFICE SYMBOL

DD FORM 1473, 84 MAR 83 APR edition may be used until exhausted. All other editions are obsolete

SECURITY CLASSIFICATION OF THIS PAGE

TECHNICAL REPORT #7

(Abstract continued)

not as accurate as those by the generalized hard-rod model which has been applied to the same problem in a previous study.

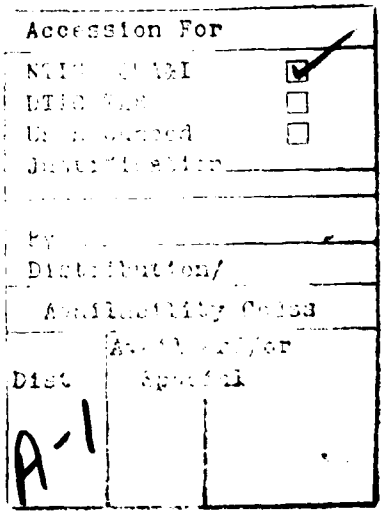

NONLOCAL FREE ENERGY DENSITY FUNCTIONAL THEORY APPLIED TO THE ELECTRICAL DOUBLE LAYER. I. SYMMETRICAL ELECTROLYTES

Zixiang Tang, L. Mier-y-Teran*, H. T. Davis, L. E. Scriven, and H. S. White

Department of Chemical Engineering and Materials Science
University of Minnesota
421 Washington Avenue S.E.
Minneapolis, Minnesota 55455
U. S. A.

Runing Title: Electrical Double Layer

* On sabbatical leave from Departamento de Fisica, Universidad Autonoma Metropolitana-Iztapalapa, Apartado Postal 55-534, 09340 Mexico, D. F., Mexico.

ABSTRACT

A theoretical study of the restricted primitive model of the electrical double layer using a free energy density functional theory is presented. The ion-ion hard-core repulsive contribution to the free energy is incorporated by a nonlocal excess hard-sphere free energy density functional. The electrostatic part of the ion-ion direct correlation function of the inhomogeneous electrolyte in the interfacial region is approximated by that of the homogeneous bulk electrolyte. The generalized van der Waals model and the Tarazona model are used to construct the respective excess hard-sphere free energy density functionals and compared with each other. Each model requires as input a hard-sphere equation of state. The Carnahan-Starling equation of state is chosen. The theory predicts correctly the layering effect of the counterions and the charge inversion phenomenon. The results for 1:1 and 2:2 electrolytes agree well with the Monte Carlo simulations. The Tarazona model gives results in closer agreement with Monte Carlo data than does the generalized van der Waals model. The diffuse layer potentials predicted by the Tarazona model are not as accurate as those by the generalized hard-rod model which has been applied to the same problem in a previous study.

I. INTRODUCTION

The electrical double layer is the inhomogeneous region of an electrolyte near a charged surface. Its most distinguishing feature is the charge separation in the electrolyte in response to the electric field produced by the surface charges. Understanding the electrical double layer is fundamental to a variety of phenomena in electrochemical, colloid, and biological sciences.

Because of many complications present in physical systems containing the electrical double layers, theoretical studies have concentrated largely on some simplified models. The advantage in using a simplified model is that it allows an unambiguous test of a theory against the computer simulations for the same model. Among these models, the most widely studied one is the restricted primitive model (RPM), in which the electrolyte is represented by a fluid of charged hard spheres with diameter d and point charges q_α at their centers, the solvent by a continuum with an isotropic dielectric constant ϵ, and the electrode by an infinite planar hard wall with a uniform surface charge density σ. The electrode surface is also assumed to be impenetrable. The RPM of the electrical double layer is completely defined once the system parameters ϵ, σ, d, $\{q_\alpha\}$, the ion number densities in the bulk electrolyte $\{n_\alpha^0\}$, and the temperature T are specified.

Studies of the RPM of the electrical double layer began with the pioneering works of Gouy [1] and Chapman [2] based on the Poisson-Boltzmann equation, in which the ions were treated as point charges so that the hard-core repulsions between the ions and between the ion and the charged wall were not included. A modification was made later by Stern [3] to incorporate the ionic size effects in such a way that all ions were allowed to approach only up to a closest distance from the charged surface, whereas the ion-ion interactions were still treated by the point charge model. This was called the modified Gouy-Chapman (MGC) theory [1-3]. The MGC theory is quantitatively accurate for weakly coupled (say, small σ and q_α) systems at low densities, in which case the effects of finite ion sizes are not important, but fails to represent, even qualitatively, highly coupled systems or high density

ones. Qualitatively, there are two fundamentally important phenomena present in the ion density profiles of the RPM of the electrical double layer as revealed by the Monte Carlo (MC) simulations of Torrie and Valleau [4]: the layering effect of the counterions, and the charge inversion. Firstly, for 1:1 electrolytes near a highly charged surface the counterion density profile is no longer monotone but shows a second layer next to the inner monolayer. Secondly, for 1:1 and 2:2 electrolytes at high concentrations and high surface charges there is charge inversion, i.e., the coion density exceeds the counterion density within certain parts of the interfacial region. The MGC theory, however, always predicts monotonic profiles of the ion density [5]. Accordingly, various efforts have been directed toward interpreting of the layering and the charge inversion effects through better treatments of both the short-ranged hard-sphere interaction and the long-ranged Coulombic interaction in the electrical double layer [5,6]. These efforts include works based on the modified Poisson-Boltzmann (MPB), the Yvon-Born-Green (YBG), and the Ornstein-Zernike (OZ) equations. There are also works based on free energy density functional theories. We sketch in Table I these different theories of the RPM of the electrical double layer. For detailed references, see the recent reviews [5,6] of this subject and a recent paper by some of the present authors [19].

The MPB theory is based on the Kirkwood hierarchy and requires a closure which connects the density distribution functions and the mean electrostatic potential function. Computations based on this theory have proved efficient [5]. The best and most recent version of the MPB theory is the MPB5 theory of Outhwaite and Bhuiyan [7], which is successful for 1:1 electrolytes but not for 2:1 and 2:2 electrolytes at similar densities and temperatures. The YBG theory has a conspicuous feature: it satisfies the contact theorem exactly. For closure, this theory requires approximations to the pair distribution function. A promising nonlocal closure has been proposed recently [8]. The results of the YBG theory are good at high concentrations but poor for dilute solutions; this is believed to result from numerical difficulties when the density profiles become very long-ranged in the low concentration limit [8]. The OZ equation together with the mean spherical approximation (MSA) or the hypernetted-chain (HNC) approximation underlies the MSA/MSA,

the HNC/MSA, and the HNC/HNC theories, of which the HNC/MSA is the best. In the various versions of this theory, the ion-ion direct correlation function of the inhomogeneous electrolyte in the interface is approximated by that of the homogeneous bulk electrolyte. Numerical predictions from the HNC theories require large computational efforts, but these theories have the advantage that they can be generalized easily.

Two recent works on the extensions of the HNC theories of the RPM of the electrical double layer warrant mention. One is the local HNC (HNCL) and the local MSA (MSAL) approximations suggested by Forstmann *et al.* [9], who derived an integral equation for the density distribution functions from a density functional theory, in which the nonuniform Ornstein-Zernike direct correlation function should be approximated. The essence of these approximations is that the exact ion-ion direct correlation function of the inhomogeneous electrolytes is replaced locally by either the HNC or the MSA solutions to the direct correlation functions of some homogeneous non-neutral electrolytes. These non-neutral electrolytes are chosen in such a way that they have the ion compositions corresponding respectively to those found locally in different regions of the double layer [9]. These theories give good results, but an unsatisfactory feature of these approaches is that they have one undetermined parameter which must be fitted to the MC simulations. The other recent extension of the HNC theories is that of Plischke and Henderson [10], who solved the inhomogeneous OZ equation in the HNC and the MSA closures simultaneously with the Lovett-Mou-Buff-Wertheim equation for the ionic density profiles (OZ/LMBW). The OZ/LMBW theory gives the most accurate predictions currently available. However, its numerical implementation involves rather large computing time and considerable storage. In summary, all the theories mentioned above succeed quite well for weakly coupled systems at low densities, whereas only the YBG, the HNCL and MSAL, and the OZ/LMBW theories predict correctly the qualitative behavior of highly coupled systems at moderate or high densities. Quantitative agreement with the MC results is accomplished without adjustable parameters only by the OZ/LMBW theory.

In contrast with the approaches mentioned above, there are far fewer investigations

based on the density functional theories. The essence of the density functional theory is to construct the Helmholtz free energy as a functional of the particle density and minimize the free energy to obtain an expression for the equilibrium density distribution. In the currently tractable versions of this approach, the contribution of particle-particle pair interactions to the free energy are separated into hard-sphere and electrostatic parts. The hard-core repulsion between the ions is represented by a nonlocal generic free energy density functional for inhomogeneous hard-sphere fluids, which was first proposed by Percus [11] and generalized to fluid mixtures by Vanderlick *et al.* [12]. Several models of such a nonlocal free energy density functional have evolved in recent years. These include the generalized van der Waals (GVDW) model [13], the Tarazona (TRZ) model [14], and the generalized hard-rod model (GHRM) [15,16]. Each of these models requires as input a hard-sphere equation of state. A comparison of these models with applications to hard sphere fluids confined between hard walls has been reported [17]. The first application of the density functional theory to the RPM of the electrical double layer was the work by Boyle *et al.* [18], in which the GVDW model together with the Clausius equation of state was used and the electrostatic interaction between the ions was treated in the mean field approximation. The results obtained compare somewhat poorly with the MC simulations. This can be attributed in part to two facts: the Clausius equation of state does not account well for the behavior of a hard sphere fluid; and the mean field approximation is too crude to represent accurately the electrostatic correlations. Recently, Mier-y-Teran *et al.* [19] have applied the GHRM together with the Carnahan-Starling equation of state to the same problem. An improved treatment of the electrostatic interaction was used, in which the electrostatic part of the ion-ion direct correlation function of the inhomogeneous electrolyte in the interfacial region was approximated by that of the homogeneous bulk electrolyte. This electrostatic correlation consists of a long-ranged mean field part and a short-ranged residual part. Also, the volume averaging technique of Ref. 18 as it applied to regions very close to the charged surface, which is now believed inappropriate, has been eliminated. The GHRM has an accuracy approaching in some cases that of the OZ/LMBW theory, which is the best available, but requires only a small fraction of the computing time used to solve the OZ/LMBW theory. This is in general an attractive feature of the density

functional theory, especially in the light of the eventual goal of treating the solvent as a molecular fluid instead of a dielectric continuum.

It has been shown that the TRZ model is, overall, a better approximation for the inhomogeneous hard-sphere fluids than the GHRM [17], and that the GHRM predicts qualitatively correct results for the RPM of the electrical double layer although there are small quantitative differences from the MC data [19]. A next logical step in the development of density functional theory is to examine the accuracy of the TRZ model in applications to the RPM of the electrical double layer. The purpose of this paper is to carry out such an examination.

In section II, we use the nonlocal free energy density functional theory to derive an integral equation for the ion density distribution functions of the RPM of the electrical double layer. We extend the TRZ model to mixtures of hard spheres of the same size and then apply it together with the Carnahan-Starling equation of state to construct the excess hard-sphere free energy functional. Because of its simplicity, the GVDW model, which is in fact the lowest order approximation to the TRZ model, is also examined. The approach we use is the same as that in Ref. 19. The results for the ion density profiles and the mean electrostatic potential profiles are reported in Sec. III, and compared with the MC simulations [4] and the results of other theories, especially those of Ref. 19. In Sec. IV, we conclude with a brief summary and suggest improvements on the present approach. We also mention the extensions of the density functional theory to more realistic models of the electrical double layer.

II. THEORY

A general starting point for the treatment of the inhomogeneous fluids is the density functional theory in which the Helmholtz free energy F is expressed as a functional of the particle density distribution $n(\mathbf{r})$ [20,21]. For a system of charged particles of different

kinds α ($\alpha = 1, 2, \ldots, m$) at fixed temperature T, volume, the external field of potentials $v_\alpha(\mathbf{r})$, and the chemical potentials μ_α, the equilibrium particle density distribution is that which minimizes the grand potential Ω of the system where

$$\Omega(\{\mathbf{n}\}) = F(\{\mathbf{n}\}) - \sum_\alpha \int d^3r \mu_\alpha n_\alpha(\mathbf{r}). \tag{2.1}$$

The equilibrium particle density distribution is thus a solution to the following Euler-Lagrange equation resulting from the minimization of $\Omega(\{\mathbf{n}\})$ with respect to $n_\alpha(\mathbf{r})$:

$$\frac{\delta\Omega(\{\mathbf{n}\})}{\delta n_\alpha(\mathbf{r})} \equiv \frac{\delta F(\{\mathbf{n}\})}{\delta n_\alpha(\mathbf{r})} - \mu_\alpha = 0. \tag{2.2}$$

The Helmholtz free energy density functional of the system mentioned above is assumed to be written as

$$\begin{aligned} F(\{\mathbf{n}\}) = kT \sum_\alpha \int d^3r\, n_\alpha(\mathbf{r}) \left[ln \left(\Lambda_\alpha^3 n_\alpha(\mathbf{r}) \right) - 1 \right] \\ + \sum_\alpha \int d^3r\, n_\alpha(\mathbf{r}) v_\alpha(\mathbf{r}) - \phi(\{\mathbf{n}\}), \end{aligned} \tag{2.3}$$

where k is Boltzmann's constant and Λ_α denotes the de Broglie wavelength of particles of species α. The first term on the right side of Eq. (2.3) is the ideal gas contribution to the free energy. The second term corresponds to the external field contribution. The third term, the functional $-\phi(\{\mathbf{n}\})$, represents the contributions from the ion-ion pair interactions. The functional $\phi(\{\mathbf{n}\})$ is a unique functional of particle density in a specific system and its derivatives with respect to density define a hierarchy of direct correlation functions [20,21]. Of particular importance, the nonuniform Ornstein-Zernike direct correlation function $c_{\alpha\beta}(\mathbf{r}, \mathbf{r}')$ is given by

$$c_{\alpha\beta}(\mathbf{r}, \mathbf{r}') = \frac{1}{kT} \frac{\delta^2 \phi(\{\mathbf{n}\})}{\delta n_\alpha(\mathbf{r}) \delta n_\beta(\mathbf{r}')}. \tag{2.4}$$

If we have some means of evaluating the direct correlation functions over a range of nonuniform densities, we can obtain $\phi(\{\mathbf{n}\})$ by functional integrations of the direct correlation functions with respect to density.

Although $\phi(\{\mathbf{n}\})$ does not depend on the specific choice of integration path [20], it is most convenient to integrate along a linear density path from some initial density $n'_\alpha(\mathbf{r})$ to the final density $n_\alpha(\mathbf{r})$,

$$n_\alpha(\mathbf{r};\lambda) = n'_\alpha(\mathbf{r}) + \lambda\left[n_\alpha(\mathbf{r}) - n'_\alpha(\mathbf{r})\right], \tag{2.5}$$

where λ is a parameter varying between 0 and 1. Such an integration can be further simplified if the initial density is chosen to be zero, $n'_\alpha(\mathbf{r}) = 0$. Because the particle-particle pair interactions become negligible at sufficiently low density, we have $\phi(\{\mathbf{n}'\}) = 0$ in this case [21]. This yields

$$\phi(\{\mathbf{n}\}) = kT\sum_{\alpha\beta}\int\int d^3r\, d^3r'\, n_\alpha(\mathbf{r})n_\beta(\mathbf{r}')\int_0^1 d\lambda\int_0^\lambda d\lambda'\, c_{\alpha\beta}(\mathbf{r},\mathbf{r}';\lambda'). \tag{2.6}$$

A reference (initial) state different from that used in Ref. 19 has been chosen here in the expression of the density functional ϕ, but the equivalence of the two approaches is guaranteed by the uniqueness of ϕ.

The free energy density functional then becomes

$$\begin{aligned} F(\{\mathbf{n}\}) = {} & kT\sum_\alpha\int d^3r\, n_\alpha(\mathbf{r})\left[ln\left(\Lambda_\alpha^3 n_\alpha(\mathbf{r})\right) - 1\right] \\ & + \sum_\alpha\int d^3r\, n_\alpha(\mathbf{r})v_\alpha(\mathbf{r}) \\ & - kT\sum_{\alpha\beta}\int\int d^3r\, d^3r'\, n_\alpha(\mathbf{r})n_\beta(\mathbf{r}')\int_0^1 d\lambda\int_0^\lambda d\lambda'\, c_{\alpha\beta}(\mathbf{r},\mathbf{r}';\lambda'). \end{aligned} \tag{2.7}$$

It bears emphasizing that in this paper we employ the Helmholtz free energy density functional rather than the grand potential functional which was used in Ref. 19. These two functionals are simply related to each other by Eq. (2.1). No approximations have been made so far concerning the physical system we are going to investigate, and in this sense Eq. (2.7) is exact.

For an inhomogeneous RPM electrolyte with both hard-core repulsions and Coulombic interactions, the nonuniform Ornstein-Zernike direct correlation function $c_{\alpha\beta}(\mathbf{r},\mathbf{r}')$ is

not in general known. But it can be decomposed into three parts:

$$c_{\alpha\beta}(\mathbf{r},\mathbf{r}') = c^{hs}_{\alpha\beta}(\mathbf{r},\mathbf{r}') - \frac{q_\alpha q_\beta}{\epsilon kT|\mathbf{r}-\mathbf{r}'|} + \Delta c_{\alpha\beta}(\mathbf{r},\mathbf{r}'). \tag{2.8}$$

The first term on the right side of Eq.(2.8), $c^{hs}_{\alpha\beta}(\mathbf{r},\mathbf{r}')$, is the direct correlation function of a fluid of neutral hard spheres due solely to hard-core repulsion, which is discussed in more detail in what follows. The second term represents the ionic correlation due solely to the Coulombic interaction between charged particles. Here we have made an additional assumption about the RPM of the electrical double layer: the electrode surface is taken as having the same dielectric constant ϵ as has the solvent. In this case there are no image effects arising from the polarizations of the surface, and the electrostatic interaction between ions remains in the form of central force as expressed by Eq.(2.8). An additional contribution in the same equation, $\Delta c_{\alpha\beta}(\mathbf{r},\mathbf{r}')$, can be interpreted in some sense as the results of the cross-correlations between the Coulombic and the hard-sphere interactions. To proceed further we must make some kinds of approximations for $c^{hs}_{\alpha\beta}(\mathbf{r},\mathbf{r}')$ and $\Delta c_{\alpha\beta}(\mathbf{r},\mathbf{r}')$. We choose here to approximate $\Delta c_{\alpha\beta}(\mathbf{r},\mathbf{r}')$ of the inhomogeneous electrolyte in the interface by that of the homogeneous neutral bulk electrolyte, $\Delta c_{\alpha\beta}(|\mathbf{r}-\mathbf{r}'|)$. The latter is given by the analytical solution to the OZ equation when the MSA closure is used [22]. The explicit expression for $\Delta c_{\alpha\beta}(|\mathbf{r}-\mathbf{r}'|)$ is given in Ref. 19.

On the other hand, instead of making any kind of explicit approximation to the hard-sphere correlation function $c^{hs}_{\alpha\beta}(\mathbf{r},\mathbf{r}')$, we introduce an excess free energy density functional $F^{excess}(\{\mathbf{n}\})$ into our formalism to incorporate the hard-core repulsion between the ions. $F^{excess}(\{\mathbf{n}\})$ is essentially the excess free energy of a hard sphere fluid over the ideal gas contribution accounting for the finite size of the particles. This excess part of the free energy is extremly important in determining the structure of Coulombic and non-Coulombic inhomogeneous fluids provided there is short-ranged hard-core repulsion between the particles.

On the basis of all the foregoing, the free energy density functional can be rewritten

as

$$
\begin{aligned}
F(\{\mathbf{n}\}) = kT \sum_{\alpha} \int d^3r\, n_\alpha(\mathbf{r}) \left[ln\left(\Lambda_\alpha^3 n_\alpha(\mathbf{r})\right) - 1 \right] \\
+ \sum_{\alpha} \int d^3r\, n_\alpha(\mathbf{r}) v_\alpha(\mathbf{r}) \\
+ \frac{1}{2} \sum_{\alpha\beta} \int\int d^3r\, d^3r'\, n_\alpha(\mathbf{r}) n_\beta(\mathbf{r}') \frac{q_\alpha q_\beta}{\epsilon |\mathbf{r} - \mathbf{r}'|} \\
- \frac{1}{2} kT \sum_{\alpha\beta} \int\int d^3r\, d^3r'\, n_\alpha(\mathbf{r}) n_\beta(\mathbf{r}') \Delta c_{\alpha\beta}(|\mathbf{r} - \mathbf{r}'|) \\
+ F^{excess}(\{\mathbf{n}\}).
\end{aligned}
\tag{2.9}
$$

Here the external field potential $v_\alpha(\mathbf{r})$ in the planar electrical double layer can be shown to be [5]

$$
v_\alpha(\mathbf{r}) = -2\pi q_\alpha \sigma x/\epsilon + v^{hs}(x), \tag{2.10}
$$

where $x \equiv |\mathbf{r} \cdot \hat{\mathbf{x}}|$ is the ion's distance to the wall,

$$
\begin{aligned}
v^{hs}(x) &= \infty, \qquad x < d/2, \\
&= 0, \qquad x > d/2.
\end{aligned}
\tag{2.11}
$$

As an intuitive generalization of the exact theory of the inhomogeneous hard-rod fluids, the excess hard-sphere free energy functional $F^{excess}(\{\mathbf{n}\})$ suggested by Percus is in general a nonlocal density functional and can be expressed in terms of two coarse-grained densities, $\bar{n}_\alpha^\nu(\mathbf{r})$ and $\bar{n}_\alpha^\tau(\mathbf{r})$, which are themselves at each point density functionals of the local density distribution $n_\alpha(\mathbf{r})$:

$$
F^{excess}(\{\mathbf{n}\}) = \sum_{\alpha} \int d^3r\, \bar{n}_\alpha^\nu(\mathbf{r}) \mathcal{F}_0\left(\bar{\mathbf{n}}^\tau(\mathbf{r})\right), \tag{2.12}
$$

where $\mathcal{F}_0(n)$ is the excess free energy per particle of a homogeneous hard sphere fluid of density n, and its expression can be derived from the hard-sphere equation of state [10,11]. The physical interpretation of Eq.(2.12) is that the excess free energy contributed from a unit volume around $\mathbf{r}$ is the product of two quantities: the *average* number density of particles, $\bar{n}^\nu(\mathbf{r})$, and the *average* excess free energy per particle which is simply replaced by the excess free energy per particle of a homogeneous hard-sphere fluid of the *average*

density $\bar{n}^{\tau}(\mathbf{r})$. These two average densities (or coarse-grained densities) are not necessarily identical.

We choose here to use the Carnahan-Starling equation of state in our calculations. The corresponding excess hard-sphere free energy per particle is

$$\mathcal{F}_0(n) = kT\frac{y(4-3y)}{(1-y)^2}, \tag{2.13}$$

where $y \equiv \pi n d^3/6$. The expression for $\mathcal{F}_0(n)$ retains its simple form as in Eq. (2.13) when extended to mixtures of hard spheres of equal size if we identify n with the total number density of particles of all species, i.e., $n = \sum_\alpha n_\alpha$.

In the expression for the excess hard-sphere free energy density functional, Eq.(2.12), the coarse-grained densities, $\bar{n}^{\nu}_{\alpha}(\mathbf{r})$ and $\bar{n}^{\tau}_{\alpha}(\mathbf{r})$, are the weighted-averages of the local density over certain spatial domains whose sizes are comparable to the particle volumes. This is

$$\bar{n}^{\nu}_{\alpha}(\mathbf{r}) \equiv \int d^3r'\, n_\alpha(\mathbf{r}')\nu_\alpha(\mathbf{r}-\mathbf{r}';\{\mathbf{n}\}), \tag{2.14}$$

$$\bar{n}^{\tau}_{\alpha}(\mathbf{r}) \equiv \int d^3r'\, n_\alpha(\mathbf{r}')\tau_\alpha(\mathbf{r}-\mathbf{r}';\{\mathbf{n}\}), \tag{2.15}$$

where the weighting functions, ν and τ, are required to satisfy the normalization conditions

$$\int d^3r'\, \nu_\alpha(\mathbf{r}-\mathbf{r}';\{\mathbf{n}\}) = \int d^3r'\, \tau_\alpha(\mathbf{r}-\mathbf{r}';\{\mathbf{n}\}) = 1, \tag{2.16}$$

since these coarse-grained densities both reduce to the bulk density in the homogeneous fluid limit.

In order to complete the construction of the excess free energy functional, prescriptions for the weighting functions must be specified. Different prescriptions define different models in free energy density functional theory. The simplest criterion used to determine the "optimal" weighting functions, ν and τ, is that they should reproduce the known results of the hard-sphere fluids in the uniform density limit. For example, we can require both the Ornstein-Zernike direct correlation function and its first derivative with respect

to the density to be reproduced [11]. The first free energy density functional model which incorporated coarse-grained densities was the generalized van der Waals (GVDW) model of Nordholm and co-workers [13]. The weighting functions of this model are

$$\nu_\alpha(\mathbf{r}-\mathbf{r}';\{\mathbf{n}\}) = \delta(\mathbf{r}-\mathbf{r}'), \tag{2.17}$$

and

$$\begin{aligned} \tau_\alpha(\mathbf{r}-\mathbf{r}';\{\mathbf{n}\}) &= \frac{3}{4\pi d^3}, \qquad |\mathbf{r}-\mathbf{r}'| < d, \\ &= 0, \qquad\qquad |\mathbf{r}-\mathbf{r}'| > d, \end{aligned} \tag{2.18}$$

where $\delta(\mathbf{r})$ is the Dirac delta function. The GVDW theory was found to predict physically unrealistic behavior of inhomogeneous hard sphere fluids at high densities [14,17], and unsatisfactory results in the case of the RPM of the electrical double layer [18].

There is another free energy density functional model, the generalized hard-rod model (GHRM), proposed by Robledo and Varea [15], and by Fischer and Heinbuch [16]. The GHRM is the three-dimensional generalization of the one-dimensional hard-rod model and is defined by

$$\nu_\alpha(\mathbf{r}-\mathbf{r}';\{\mathbf{n}\}) = \frac{1}{4\pi(d/2)^2}\delta(d/2-|\mathbf{r}-\mathbf{r}'|), \tag{2.19}$$

and

$$\begin{aligned} \tau_\alpha(\mathbf{r}-\mathbf{r}';\{\mathbf{n}\}) &= \frac{3}{4\pi(d/2)^3}, \qquad |\mathbf{r}-\mathbf{r}'| < d/2, \\ &= 0, \qquad\qquad |\mathbf{r}-\mathbf{r}'| > d/2, \end{aligned} \tag{2.20}$$

The counterparts of Eqs.(2.19) and (2.20) are exact in the one-dimensional case. It has been shown that the GHRM predicted qualitatively correct but quantitatively poor results for hard-sphere fluids confined between two hard walls [17]. Yet the results of the GHRM for the RPM of the electrical double layer were found to be satisfactory, and even quantitatively accurate in many cases [19].

Improvements on the GVDW theory have been made by Tarazona [14] through introducing a density-dependent weighting function $\tau(\mathbf{r}-\mathbf{r}';\{\mathbf{n}\})$. The other weighting function $\nu(\mathbf{r}-\mathbf{r}';\{\mathbf{n}\})$, however, has remained a Dirac delta function. In the TRZ model,

τ is assumed to expand in a power series in the coarse-grained density $\bar{n}^{\tau}$, and the series is truncated at the third term:

$$\tau(\mathbf{r}-\mathbf{r}';\{\mathbf{n}\}) \approx w^{(0)}(|\mathbf{r}-\mathbf{r}'|)+w^{(1)}(|\mathbf{r}-\mathbf{r}'|)\bar{n}^{\tau}(\mathbf{r})+w^{(2)}(|\mathbf{r}-\mathbf{r}'|)\bar{n}^{\tau}(\mathbf{r})^2, \qquad (2.21)$$

where $w^{(i)}(r)$ $(i=0,1,2)$ are density-independent coefficients. The coefficients of the zeroth- and first-order terms, $w^{(0)}(r)$ and $w^{(1)}(r)$, were determined by comparison with the virial expansion of the direct correlation function of a uniform hard sphere fluid. The coefficient of the second-order term, $w^{(2)}(r)$, was calculated through an empirical fit to the Percus-Yevick approximation of the direct correlation function [14]. In addition, the normalization condition for $\tau(\mathbf{r}-\mathbf{r}';\{\mathbf{n}\})$, Eq. (2.16), implies that $w^{(0)}(r)$ is normalized, and that $w^{(1)}(r)$ and $w^{(2)}(r)$ have zero integrals:

$$\begin{aligned} \int d^3r\, w^{(i)}(|\mathbf{r}|) &= 1, \qquad i=0, \\ &= 0, \qquad i=1,2. \end{aligned} \qquad (2.22)$$

The coefficients $w^{(i)}(r)$ obtained in this manner are optimized. The results are

$$\begin{aligned} w^{(0)}(r) &= \frac{3}{4\pi d^3}, \qquad r<d, \\ &= 0, \qquad r>d, \end{aligned} \qquad (2.23a)$$

$$\begin{aligned} w^{(1)}(r) &= 0.475-0.648\left(\frac{r}{d}\right)+0.113\left(\frac{r}{d}\right)^2, && r<d, \\ &= 0.288\left(\frac{d}{r}\right)-0.924+0.764\left(\frac{r}{d}\right)-0.187\left(\frac{r}{d}\right)^2, && d<r<2d, \\ &= 0, && r>2d, \end{aligned} \qquad (2.23b)$$

$$\begin{aligned} w^{(2)}(r) &= \frac{5\pi d^3}{144}\left[6-12\left(\frac{r}{d}\right)+5\left(\frac{r}{d}\right)^2\right], && r<d, \\ &= 0, && r>d. \end{aligned} \qquad (2.23c)$$

One realizes immediately that the GVDW model is just the zeroth order approximation to the TRZ model by comparing Eqs.(2.18) and (2.23). The TRZ model combined with the Carnahan-Starling equation of state was found to predict the best results among those three models we discussed for hard-sphere fluids confined between two hard walls [17].

Extending the TRZ model to mixtures of hard spheres with arbitary size ratio involves large complexities [23]; the power series expansion of the weighting function τ is thus

truncated at the linear term in density as has been done in Ref. 23. In the case of mixtures of hard spheres with the same size, however, the TRZ model is much easier to be extended. Because only the particle diameter determines the finite size effects, regardless of the other parameters such as charge, it is reasonable to assume that for mixtures of hard spheres of equal size the weighting functions, $\nu_\alpha(\mathbf{r}-\mathbf{r}';\{\mathbf{n}\})$ and $\tau_\alpha(\mathbf{r}-\mathbf{r}';\{\mathbf{n}\})$, are independent of the particle species α and take the forms

$$\nu_\alpha(\mathbf{r}-\mathbf{r}';\{\mathbf{n}\}) = \delta(\mathbf{r}-\mathbf{r}'), \tag{2.24}$$

and

$$\begin{aligned}\tau_\alpha(\mathbf{r}-\mathbf{r}';\{\mathbf{n}\}) = w^{(0)}(|\mathbf{r}-\mathbf{r}'|) + w^{(1)}(|\mathbf{r}-\mathbf{r}'|)\sum_\beta \bar{n}^\tau_\beta(\mathbf{r}) \\ + w^{(2)}(|\mathbf{r}-\mathbf{r}'|)\sum_{\beta\gamma}\bar{n}^\tau_\beta(\mathbf{r})\bar{n}^\tau_\gamma(\mathbf{r}),\end{aligned} \tag{2.25}$$

where the coefficients $w^{(i)}(r)$ are given by Eq. (2.23). Eq. (2.25) is essentially the same as Eq. (2.21) except that the coarse-grained density $\bar{n}^\tau(\mathbf{r})$ is now identified with the total coarse-grained density of particles of all species, $\sum_\beta \bar{n}^\tau_\beta(\mathbf{r})$. It follows from Eqs. (2.15) and (2.25) that

$$\bar{n}^\tau_\alpha(\mathbf{r}) = \bar{n}^{(0)}_\alpha(\mathbf{r}) + \bar{n}^{(1)}_\alpha(\mathbf{r})\bar{n}^\tau(\mathbf{r}) + \bar{n}^{(2)}_\alpha(\mathbf{r})\bar{n}^\tau(\mathbf{r})^2, \tag{2.26}$$

where

$$\bar{n}^{(i)}_\alpha(\mathbf{r}) = \int d^3r'\, n_\alpha(\mathbf{r}')w^{(i)}(|\mathbf{r}-\mathbf{r}'|), \quad i=0,1,2, \tag{2.27}$$

and

$$\bar{n}^\tau(\mathbf{r}) = \sum_\beta \bar{n}^\tau_\beta(\mathbf{r}). \tag{2.28}$$

Summing over all the equations of (2.26) for all species α yields

$$\bar{n}^\tau(\mathbf{r}) = \bar{n}^{(0)}(\mathbf{r}) + \bar{n}^{(1)}(\mathbf{r})\bar{n}^\tau(\mathbf{r}) + \bar{n}^{(2)}(\mathbf{r})\bar{n}^\tau(\mathbf{r})^2, \tag{2.29}$$

where

$$\bar{n}^{(i)}(\mathbf{r}) = \sum_\beta \bar{n}^{(i)}_\beta(\mathbf{r}). \tag{2.30}$$

Eq. (2.29) can then be solved for $\bar{n}^{\tau}(\mathbf{r})$ to give

$$\bar{n}^{\tau}(\mathbf{r}) = 2\bar{n}^{(0)}(\mathbf{r}) \left\{ \left(1 - \bar{n}^{(1)}(\mathbf{r})\right) + \left[\left(1 - \bar{n}^{(1)}(\mathbf{r})\right)^2 - 4\bar{n}^{(0)}(\mathbf{r})\bar{n}^{(2)}(\mathbf{r}) \right]^{\frac{1}{2}} \right\}^{-1}. \tag{2.31}$$

Eqs. (2.26) and (2.31) together determine the coarse-grained density $\bar{n}^{\tau}_{\alpha}(\mathbf{r})$, and it is clear that they reduce to Tarazona's results [13] in the case of single-component hard sphere system.

It is worthwhile deriving the functional derivatives of the coarse-grained densities with respect to the local density for the TRZ model. The results are

$$\frac{\delta \bar{n}^{\nu}_{\beta}(\mathbf{r}')}{\delta n_{\alpha}(\mathbf{r})} = \delta_{\alpha\beta}\delta(\mathbf{r}' - \mathbf{r}), \tag{2.32}$$

$$\frac{\delta \bar{n}^{\tau}(\mathbf{r}')}{\delta n_{\alpha}(\mathbf{r})} = \frac{\tau(\mathbf{r}' - \mathbf{r}; \bar{n}^{\tau}(\mathbf{r}'))}{1 - \bar{n}^{(1)}(\mathbf{r}') - 2\bar{n}^{(2)}(\mathbf{r}')\bar{n}^{\tau}(\mathbf{r}')}, \tag{2.33}$$

and

$$\begin{aligned} \frac{\delta \bar{n}^{\tau}_{\beta}(\mathbf{r}')}{\delta n_{\alpha}(\mathbf{r})} = \frac{\delta \bar{n}^{\tau}(\mathbf{r}')}{\delta n_{\alpha}(\mathbf{r})} \Big\{ & \delta_{\alpha\beta} - \left[\bar{n}^{(1)}(\mathbf{r}')\delta_{\alpha\beta} - \bar{n}^{(1)}_{\beta}(\mathbf{r}')\right] \\ & - 2\bar{n}^{\tau}(\mathbf{r}') \left[\bar{n}^{(2)}(\mathbf{r}')\delta_{\alpha\beta} - \bar{n}^{(2)}_{\beta}(\mathbf{r}')\right] \Big\}, \end{aligned} \tag{2.34}$$

where $\delta_{\alpha\beta}$ is the Kronecker delta function.

Combining together all the contributions to the Helmholtz free energy density functional $F(\{\mathbf{n}\})$ in Eq.(2.9) yields

$$\begin{aligned} F(\{\mathbf{n}\}) = & kT \sum_{\alpha} \int d^3r\, n_{\alpha}(\mathbf{r}) \left[ln\left(\Lambda^3_{\alpha} n_{\alpha}(\mathbf{r})\right) - 1\right] \\ & + \sum_{\alpha} \int d^3r\, n_{\alpha}(\mathbf{r}) v_{\alpha}(\mathbf{r}\ ) \\ & + \sum_{\alpha} \int d^3r\, \bar{n}^{\nu}_{\alpha}(\mathbf{r}) \mathcal{F}_0(\bar{\mathbf{n}}^{\tau}(\mathbf{r})) \\ & + \frac{1}{2} \sum_{\alpha\beta} \int\int d^3r\, d^3r'\, n_{\alpha}(\mathbf{r}) n_{\beta}(\mathbf{r}') \frac{q_{\alpha} q_{\beta}}{\epsilon |\mathbf{r} - \mathbf{r}'|} \\ & - \frac{1}{2} kT \sum_{\alpha\beta} \int\int d^3r\, d^3r'\, n_{\alpha}(\mathbf{r}) n_{\beta}(\mathbf{r}') \Delta c_{\alpha\beta}(|\mathbf{r} - \mathbf{r}'|). \end{aligned} \tag{2.35}$$

The chemical potential of ions of species α in the electrical double layer is computed from Eq. (2.35) as the functional derivative of F with respect to the density of species α. This gives

$$\begin{aligned}\mu_\alpha = & kT\, ln\left(\Lambda_\alpha^3 n_\alpha(\mathbf{r})\right) + q_\alpha\psi(\mathbf{r}) + v^{hs}(\mathbf{r}) \\ & + \sum_\beta \int d^3r' \frac{\delta \bar{n}_3^\nu(\mathbf{r}')}{\delta n_\alpha(\mathbf{r})} \mathcal{F}_0(\bar{\mathbf{n}}^\tau(\mathbf{r}')) \\ & + \sum_\beta \int d^3r' \bar{n}_\beta^\nu(\mathbf{r}') \left[\sum_\gamma \frac{\delta \bar{n}_\gamma^\tau(\mathbf{r}')}{\delta n_\alpha(\mathbf{r})} \cdot \frac{\delta \mathcal{F}_0(\bar{\mathbf{n}}^\tau(\mathbf{r}'))}{\delta \bar{n}_\gamma^\tau(\mathbf{r}')}\right] \\ & - kT \sum_\beta \int d^3r'\, n_\beta(\mathbf{r}') \Delta c_{\alpha\beta}(|\mathbf{r}-\mathbf{r}'|),\end{aligned} \tag{2.36}$$

where $\psi(\mathbf{r})$ is the mean electrostatic potential defined by

$$\psi(\mathbf{r}) \equiv v^c(x) + \int d^3r' \sum_\alpha \frac{q_\alpha n_\alpha(\mathbf{r})}{\epsilon|\mathbf{r}-\mathbf{r}'|}. \tag{2.37}$$

Poisson's equation can be solved with the appropriate boundary conditions for the planar electrical double layer to give the mean electrostatic potential in terms of the ion density distribution functions [5]. The result is

$$\psi(x) = \frac{4\pi}{\epsilon} \int_x^\infty dx'(x-x') \sum_\alpha q_\alpha n_\alpha(x'). \tag{2.38}$$

Evaluating the chemical potential in the coexisting homogeneous bulk electrolyte and combining this with Eq. (2.36), we obtain an integral equation for $n_\alpha(\mathbf{r})$ as a function of temperature and bulk ion densities n_α^0. Because of the planar symmetry of the problem, the ion densities vary only in the direction normal to the surface. Integrating $\nu_\alpha(\mathbf{r}-\mathbf{r}';\{\mathbf{n}\})$, $\tau_\alpha(\mathbf{r}-\mathbf{r}';\{\mathbf{n}\})$, and $\Delta c_{\alpha\beta}(|\mathbf{r}-\mathbf{r}'|)$ over the directions parallel to the wall, i.e., the y-z

plane, leads to the one-dimensional integral equation for $n_\alpha(x)$:

$$\begin{aligned}\frac{n_\alpha(x)}{n_\alpha^0} = exp\Bigg\{ & -\frac{q_\alpha \psi(x)}{kT} \\ & - \frac{1}{kT}\sum_\beta \int dx' \, \frac{\delta \bar{n}_\beta^\nu(x')}{\delta n_\alpha(x)} \mathcal{F}_0(\bar{\mathbf{n}}^\tau(x')) + \frac{\mathcal{F}_0(\mathbf{n}^0)}{kT} \\ & - \frac{1}{kT}\sum_\beta \int dx' \, \bar{n}_\beta^\nu(x') \left[\sum_\gamma \frac{\delta \bar{n}_\gamma^\tau(x')}{\delta n_\alpha(x)} \cdot \frac{\delta \mathcal{F}_0(\bar{\mathbf{n}}^\tau(x'))}{\delta \bar{n}_\gamma^\tau(x')} \right] \\ & + \frac{n}{kT}\frac{\partial \mathcal{F}_0(\mathbf{n}^0)}{\partial n_\alpha^0} + \sum_\beta \int dx' \, (n_\beta(x') - n_\beta) \Delta c_{\alpha\beta}(x - x') \Bigg\},\end{aligned} \tag{2.39a}$$

for $x > d/2$, and

$$n_\alpha(x) = 0, \tag{2.39b}$$

for $x < d/2$, where n_α^0 is the ion number density in the bulk phase and $n^0 = \sum_\beta n_\beta^0$.

III. RESULTS

The restricted primitive model of the electrical double layer, Eq. (2.39), was solved by means of finite element techniques described elsewhere [24] to obtain the equilibrium ion density distributions of 1:1 and 2:2 electrolytes. The mean electrostatic potential function then followed immediately from Eq. (2.38). In our method, the domain of interest, $d/2 \leq x \leq L$ (L is the cutoff value for all the integrals in Eq. (2.39)), was discretized uniformly and the trapezoidal rule was used to perform all the integrations. Eq. (2.39) then becomes a system of nonlinear algebraic equations for the nodal values of the reduced density $g_{\alpha i} = n_\alpha(x_i)/n_\alpha^0$. We used Newton's iterative method to solve for the unknowns. The iterations continued until the Euclidean norm of the updates was less than 10^{-10}:

$$\left[\frac{\sum_\alpha \sum_i \left(g_{\alpha i}^{(n)} - g_{\alpha i}^{(n-1)} \right)^2}{2N} \right]^{\frac{1}{2}} < 10^{-10}, \tag{3.1}$$

where N is the number of nodes in the domain. Three to seven iterations were usually required to converge to a solution.

A family of solutions was composed of several steps in the surface charge density σ at a constant concentration c. For the lowest σ, the MGC results was used as the initial guess to the solution, whereas for the higher σ, the initialization was chosen by the method of parametric continuation [25]. The domain length we used in the calculations depended on the concentration and the valence type of the bulk electrolyte; approximately 10 times of the Debye screening length κ^{-1} ($\kappa^2 = (4\pi/\epsilon kT)\sum_\alpha n_\alpha^0 q_\alpha^2$) was usually used. The criterion employed to determine the upper limit of the domain, L, is that the ion densities at $x \geq L$ should not differ from their bulk values by more than 0.01%. The number of nodes N also varied from one concentration to another. A typical value of N was 250, which was found adequate in the sense that further refinement did not change the solution by more than 1%. With 241 nodes, for example, our program required less than 40s of Cray-2 CPU time to obtain a solution.

The accuracy of the numerical method can be measured by the degree to which the overall electroneutrality condition of the interfacial region,

$$\int_0^\infty dx' \sum_\alpha q_\alpha n_\alpha(x') + \sigma = 0, \tag{3.2}$$

is satisfied. Eq. (3.2) was satisfied to at least five significant figures, except at the lowest concentrations considered (0.01M for 1:1 electrolytes and 0.05M for 2:2 electrolytes), where it was satisfied only to four significant figures.

We used the same conditions of calculations as those of the MC simulations [4]: d is 4.25Å, ϵ is 78.5, and T is 298K. The plasma parameter is $\Gamma^* = e^2/\epsilon kTd = 1.6809$ in this case. Dimensionless quantities were used for convenience as follows. The length is in units of d, the surface charge density in units of e/d^2, $\sigma^* = \sigma d^2/e$, and the mean electrostatic potential in units of kT/e, $\psi^*(x) = e\Psi(x)/kT$, where e is the magnitude of the electronic charge.

One of the most important physical quantities in the electrical double layer is the diffuse layer potential, $\psi(0)$, which is the potential difference between the closest approach

to the charged surface, $d/2$, and infinity. It follows from Eq. (2.38) that

$$\psi(0) = -\frac{4\pi}{\epsilon}\int_0^\infty dx'\, x' \sum_\alpha q_\alpha n_\alpha(x'). \tag{3.3}$$

The position of the charged surface is shifted to $x = -d/2$ in Eq. (3.3) and in all the results to be presented hereinafter. The diffuse layer potential can be interpreted as a measure of the thickness of the electrical double layer region in which the total charge $\sum_\alpha q_\alpha n_\alpha(x)$ is locally non-zero.

1. 1:1 electrolytes

We made calculations for 1:1 electrolytes at concentrations c ranging from 0.01 to 2M and surface charge densities σ^* from 0.05 to 0.9. In Table II we report the dimensionless diffuse layer potential $\psi^*(0)$ calculated from the GVDW and the TRZ models, and present the MC data [4] and the results from the GHRM [19] for comparison. We also list the results of the MGC, MPB5 [7], and YBG [8] theories, and the OZ/LMBW results by Plischke and Henderson [10]. At low concentrations and low surface charge densities, the MPB5 theory gives values of $\psi^*(0)$ which agree best with the MC results. The MPB5 results for high c or σ^* are not available. On the other hand, the YBG, the OZ/LMBW, and the density functional theory all give results of comparable accuracies at the concentrations and charge densities we investigated.

In order to compare the three different models of the free energy density functional theory, the values of $\psi^*(0)$ of these models as a function of σ^* are plotted in Fig. 1. At low concentrations and surface charge densities, our results differ from the MC simulations by only a few percent, which is about the level of statistical uncertainty in the MC data. At high concentrations and surface charge densities, however, our values of $\psi^*(0)$ are consistently lower than the MC results. In this case the TRZ model is obviously superior to the GVDW model but poorer than the GHRM; the differences between the results and the MC values are 1-5%, 10-20%, and 20-30% for the GHRM, the TRZ model, and the GVDW model, respectively. This is contrary to the finding [17] that the TRZ model is in general a better approximation for inhomogeneous hard-sphere fluids than the GHRM.

and confirms the suggestion [19] that there is some kind of fortunate cancellation of errors when the GHRM is combined with the MSA solution to the electrostatic correlation function of the homogeneous bulk electrolytes. We should expect better results from the TRZ model than from the GHRM when an improved treatment of the ion-ion electrostatic interaction is used, since the main approximation in our calculations is the replacement of the electrostatic part of the direct correlation function of the locally non-neutral inhomogeneous electrolyte by that of the homogeneous neutral bulk electrolyte. When a neutral homogeneous electrolyte is brought next to a positively charged surface, for example, there is a surplus of the anions in the interface. The electrolyte in this region is thus non-neutral and has different electrostatic correlations from those of a neutral electrolyte. It may be possible to improve our results by using the MSA solution to the electrostatic correlation function of the homogeneous but locally non-neutral electrolytes which have the ion compositions corresponding respectively to those found locally in the double layer region. This kind of calculation was reported by Forstmann and coworkers in the so-called local MSA (MSAL) approach [9].

In Figs. 2 and 3 we present the reduced ion density $n_\alpha(x)/n_\alpha^0$ and the dimensionless mean electrostatic potential $\psi^*(x) = e\Psi(x)/kT$ profiles for c=0.1M and σ^*=0.3. At this relatively low concentration and surface charge density, the profiles predicted by the GVDW and the TRZ models are almost indistinguishable (the difference is smaller than 5%) and in good agreement with the MC predictions (10% high). The density and the potential profiles are monotonic in this case.

One of the most distinctive features of the density profiles of the electrical double layer is the layering phenomenon of the counterions near the electrode plate at sufficiently high surface charges. The layering effect is caused by the hard-core exclusion interplaying with the purely electrostatic response of the ions to the electric field. We show in Figs. 4, 5, and 6 the ion density profiles for 1:1 electrolytes at c=1M and σ^*=0.42, 0.55, and 0.7, respectively. The development of the second layer of the counterions near $x = d$ is plain as σ^* increases. We see in Fig. 6 that both the TRZ and the GVDW models predict

approximately the correct position of the second peak. In the GHRM, however, the peak is shifted closer to the wall. The magnitude of the second layer is not predicted well by any of the three models; it is severely underestimated by the GVDW model and overestimated by the GHRM.

The mean electrostatic potential profile in the same conditions as in Fig. 6 is plotted in Fig. 7. In this case, the MC simulations seem to predict a minimum in the potential, but the mininum is too shallow to be resolved from the statistical noise in the data. Our profiles are still monotonic and the deviation from the MC results is the largest at $x = 0$, that is, 15% for the TRZ model and 35% for the GVDW model.

At even higher concentrations (c=2M, for example), the MC simulations begin to show the interesting effect of charge inversion, i.e., the coion density obviously exceeds the counterion density within a certain region of the interface. The result is essentially a dipole layer. In Fig. 8 we present the ion density profiles for c=2M and σ^*=0.396. Charge inversion is seen in our profiles between $x = 1.5d$ and $3d$ approximately. In this case, the TRZ model predicts results which differ from the MC simulations by no more than 10%. As a direct consequence of the charge inversion effect, the corresponding mean electrostatic potential profile shown in Fig. 9 presentes an oscillation in the potential. The minimum predicted by the TRZ model is -0.166, which is approximately 0.14 more negative than that in the MC profile. Compared with the MC results, the position of our minimum is shifted toward the charged wall.

2. 2:2 electrolytes

The 2:2 electrolyte is known to be a more stringent test of the electrical double layer theory because the ionic interactions are much stronger than those in the 1:1 electrolyte. We computed the density and the mean electrostatic potential profiles for c=0.05 and 0.5M, and σ^* varying from 0.025 to 0.4. Some selected values of $\psi^*(0)$ are also displayed in Table II to compare with the MC data and results of other theories. Again, we plot $\psi^*(0)$ as a function of σ^* in Fig. 10. Our results show a distinct maximum in the diffuse

layer potential, as predicted by the MC simulations; but they agree only qualitatively with the MC data. The disagreement is as high as 14% at 0.05M and 28% at 0.5M. The TRZ and the GVDW models again give indistinguishable results at low σ^*.

The density profiles of a 2:2 electrolyte at c=0.5M and σ^*=0.1704 are shown in Fig. 11. There is charge inversion at this moderate concentration and surface charge density. It appears that charge inversion is easier to get with 2:2 electrolytes than with 1:1 electrolytes because of the stronger interactions between the ions and between the ion and the charged surface in divalent electrolytes.

The mean electrostatic potential profile at the same conditions as in Fig. 11 is presented in Fig. 12. The potential is oscillatory with a minimum of -0.22 at $x = 0.5d$ approximately. The minimum in our profile is 18% lower than that in the MC results.

IV. SUMMARY

Free energy density functional theory has been applied to the restricted primitive model (RPM) of the electrical double layer. The hard-core repulsive contribution to the free energy was incorporated by a nonlocal excess hard-sphere free energy density functional constructed on the generalized van der Waals (GVDW) model or the Tarazona (TRZ) model. The electrostatic part of the ion-ion correlation function of the electrolyte in the interfacial region was approximated by the mean spherical approximation (MSA) to that of the homogeneous bulk neutral electrolytes. For each model, the calculations required a hard-sphere equation of state as input. The Carnahan-Starling equation of state was used.

The free energy density functional theory predicts both the ion density and the mean electrostatic potential profiles that are in good agreement with those of the Monte Carlo (MC) simulations. The theory is able to predict correctly the layering effect of the counterions near the highly charged surface and the charge inversion phenomenon at

sufficiently high concentrations and surface charge densities. At low concentrations and surface charge densities, the GVDW and the TRZ models give almost identical results. As either the concentration or the surface charge density increases, the TRZ model is obviously superior to the GVDW model. The diffuse layer potentials predicted by the TRZ model are poorer than those by the generalized hard-rod model (GHRM) reported in Ref. 19. We expect that the theory will be improved by using the MSA solution to the electrostatic correlation function of the homogeneous non-neutral electrolytes which have the same ion compositions, respectively, as those found locally in the interface. This is a matter for future investigations.

The relative accuracy of the different theories of the RPM of the electrical double layer is mainly of theoretical interest [6], since the RPM is such a greatly simplified model. Of far greater relevance is to extend these different theories to more realistic models that take into account more and more physical features of the electrical double layer. These features include the solvent effects (electrostriction, dielectric saturation), the ion effects (ion polarizability, ion-concentration dependence of the solvent dielectric constant), the asymmetric electrolytes (size asymmetry, charge asymmetry), and the surface properties (discrete charge distributions, image forces, non-planar surfaces), etc. The simplest model which incorporates the solvent effects is the hard sphere ion-dipole mixtures (HSIDM) model [5,6], in which the solvent is represented as a fluid of hard spheres with embedded point dipoles. Although this is still a crude model of an electrolyte, it is certainly an improvement over the primitive model. The extension of the density functional theory to the HSIDM model is straightforward. It requires an extra term to incorporate the finite size effects of the solvent molecules and two extra terms to include the ion-dipole and dipole-dipole interactions in the expression of the free energy density functional. We are currently working on this model.

ACKNOWLEDGMENTS

We thank the Office of Naval Research, the National Science Foundation, and the Minnesota Supercomputer Institute for their supports of this research. One of us (LMyT) gratefully acknowledges the hospitality extended to him by the Department of Chemical Engineering and Materials Science, University of Minnesota and the partial support given to him by CONACYT, Mexico.

REFERENCES

1. Gouy, G., 1910, J. Phys., **9**, 457.
2. Chapman, D. L., 1913, Phil. Mag., **25**, 475.
3. Stern, O., 1924, Z. Elektrochem., **30**, 508.
4. Torrie, G. M., and Valleau, J. P., 1980, J. Chem. Phys., **73**, 5807; Torrie, G. M., and Valleau, J. P., 1982, J. Phys. Chem., **86**, 3251.
5. Carnie, S. L., and Torrie, G. M., 1984, Adv. Chem. Phys., **56**, 141.
6. Schmickler, W., and Henderson, D., 1986, Progr. Surf. Sci., **22**, 323.
7. Outhwaite, C. W., and Bhuiyan, L. B., 1983, J. Chem. Soc. Faraday Trans. 2, **79**, 707; Outhwaite, C. W., 1983, ibid., **79**, 1315; Outhwaite, C. W., and Bhuiyan, L. B., 1986, J. Chem. Phys., **85**,4206.
8. Caccamo, C., Pizzimenti, G., and Blum, L., 1986, J. Chem. Phys., **84**, 3327; Bruno, E., Caccamo, C., and Pizzimenti, G., 1987, ibid., **86**, 5101.
9. Nielaba, P., and Forstmann, F., 1985, Chem. Phys. Lett., **117**, 46; Nielaba, P., Alts, T., Daguanno, B., and Forstmann, F., 1986, Phys. Rev. A, **34**, 1505; Daguanno, B., Nielaba, P., Alts, T., and Forstmann, F., 1986, J. Chem. Phys., **85**, 3476; Alts, T., Nielaba, P., Daguanno, B., and Forstmann, F., 1987, Chem. Phys., **111**, 223.
10. Plischke, M., and Henderson, D., 1988, J. Chem. Phys., **88**, 2712; 1989, ibid., **90**, 5738.

11. Percus, J. K., 1981, J. Chem. Phys., **75**, 1316.

12. Vanderlick, T. K., Davis, H. T., and Percus, J. K., 1989, J. Chem. Phys., **91**, 7136.

13. Nordholm, S., Johnson, M., and Freasier, B. C., 1980, Aust. J. Chem. **33**, 2139; Hooper, M. A., and Nordholm, S., 1981, ibid., **34**, 1809; Johnson, M., and Nordholm, S., 1981, J. Chem. Phys., **75**, 1953.

14. Tarazona, P., 1985, Phys. Rev. A, **31**, 2672; Tarazona, P., Marini Bettolo Marconi, U., and Evans, R., 1987, Molec. Phys., **60**, 573.

15. Robledo, A., and Varea, C., 1981, J. Stat. Phys., **26**, 513.

16. Fischer, J., and Heinbuch, U., 1988, J. Chem. Phys., **88**, 1909.

17. Vanderlick, T. K., Scriven, L. E., and Davis, H. T., 1989, J. Chem. Phys., **90**, 2422.

18. Boyle, E. J., Scriven, L. E., and Davis, H. T., 1987, J. Chem. Phys., **86**, 2309.

19. Mier-y-Teran, L., Suh, S. H., White, H. S., and Davis, H. T., 1989, J. Chem. Phys., accepted.

20. Saam, W. F., and Ebner, C., 1977, Phys. Rev. A, **15**, 2566.

21. Evans, R., 1979, Adv. in Phys., **28**, 143.

22. Waisman, E., and Lebowitz, J. L., 1972, J. Chem. Phys., **56**, 3086.

23. Tan, Z., Marini Bettolo Marconic, U., Van Swol, F., and Gubbins, K. E., 1989, J. Chem. Phys., **90**, 3704.

24. Mier-y-Teran, L., Falls, A. H., Scriven, L. E., and Davis, H. T., 1982, Proceeding 8th Symposium of Thermophysical Properties, edited by Sengens, J. V., American Society of Mechanical Engineers, New York, Vol. **1**, pp. 45-56; Mier-y-Teran, L., Diaz-Herrera, E., Lozada-Cassou, M., and Saavedra-Barrera, R., 1989, J. Comput. Phys., **84**, 326.

25. Brown, R. A., Scriven, L. E., and Silliman, W. S., 1980, in *New approaches to nonlinear problems in dynamics*, edited by Holmes, P. J., Soc. Ind. Appl. Math., Philadelphia, pp. 298–307.

FIGURE CAPTIONS

Fig. 1 Dimensionless diffuse layer potential, $e\psi(0)/kT$, as a function of the surface charge density, $\sigma d^2/e$, for 1:1 electrolytes at c=0.01, 0.1, 1, and 2M. The solid curves, the dot curves and the dashed curves are the results of the TRZ, the GVDW and the GHRM models, respectively. The dots and the squares represent the MC data.

Fig. 2 Reduced ion density profiles, $n(x)/n^0$, for a 1:1 electrolyte at $c = 0.1$M and $\sigma^* = 0.3$. The solid curves, the dot curves and the dashed curves are the results of the TRZ, the GVDW and the GHRM models, respectively. The dots represent the MC results. The charged wall is at $x = -0.5d$.

Fig. 3 Dimensionless mean electrostatic potential profile, $e\psi(x)/kT$, for a 1:1 electrolyte at $c = 0.1$M and $\sigma^* = 0.3$. All symbols as in Fig. 2.

Fig. 4 Reduced ion density profiles, $n(x)/n^0$, for a 1:1 electrolyte at $c = 1$M and $\sigma^* = 0.42$. All symbols as in Fig. 2.

Fig. 5 Reduced ion density profiles, $n(x)/n^0$, for a 1:1 electrolyte at $c = 1$M and $\sigma^* = 0.55$. All symbols as in Fig. 2.

Fig. 6 Reduced ion density profiles, $n(x)/n^0$, for a 1:1 electrolyte at $c = 1$M and $\sigma^* = 0.70$. All symbols as in Fig. 2.

Fig. 7 Dimensionless mean electrostatic potential profile, $e\psi(x)/kT$, for a 1:1 electrolyte at $c = 1$M and $\sigma^* = 0.70$. All symbols as in Fig. 2.

Fig. 8 Reduced ion density profiles, $n(x)/n^0$, for a 1:1 electrolyte at $c = 2$M and $\sigma^* = 0.396$. All symbols as in Fig. 2.

Fig. 9 Dimensionless mean electrostatic potential profile, $e\psi(x)/kT$, for a 1:1 electrolyte at

$c = 2$M and $\sigma^* = 0.396$. All symbols as in Fig. 2.

Fig. 10 Dimensionless diffuse layer potential, $e\psi(0)/kT$, as a function of the surface charge density, $\sigma d^2/e$, for 2:2 electrolytes at c=0.05 and 0.5M. All symbols as in Fig. 1.

Fig. 11 Reduced ion density profiles, $n(x)/n^0$, for a 2:2 electrolyte at $c = 0.5$M and $\sigma^* = 0.1704$. All symbols as in Fig. 2.

Fig. 12 Dimensionless mean electrostatic potential profile, $e\psi(x)/kT$, for a 2:2 electrolyte at $c = 0.5$M and $\sigma^* = 0.1704$. All symbols as in Fig. 2.

Table I. Theories of the RPM of the electrical double layer

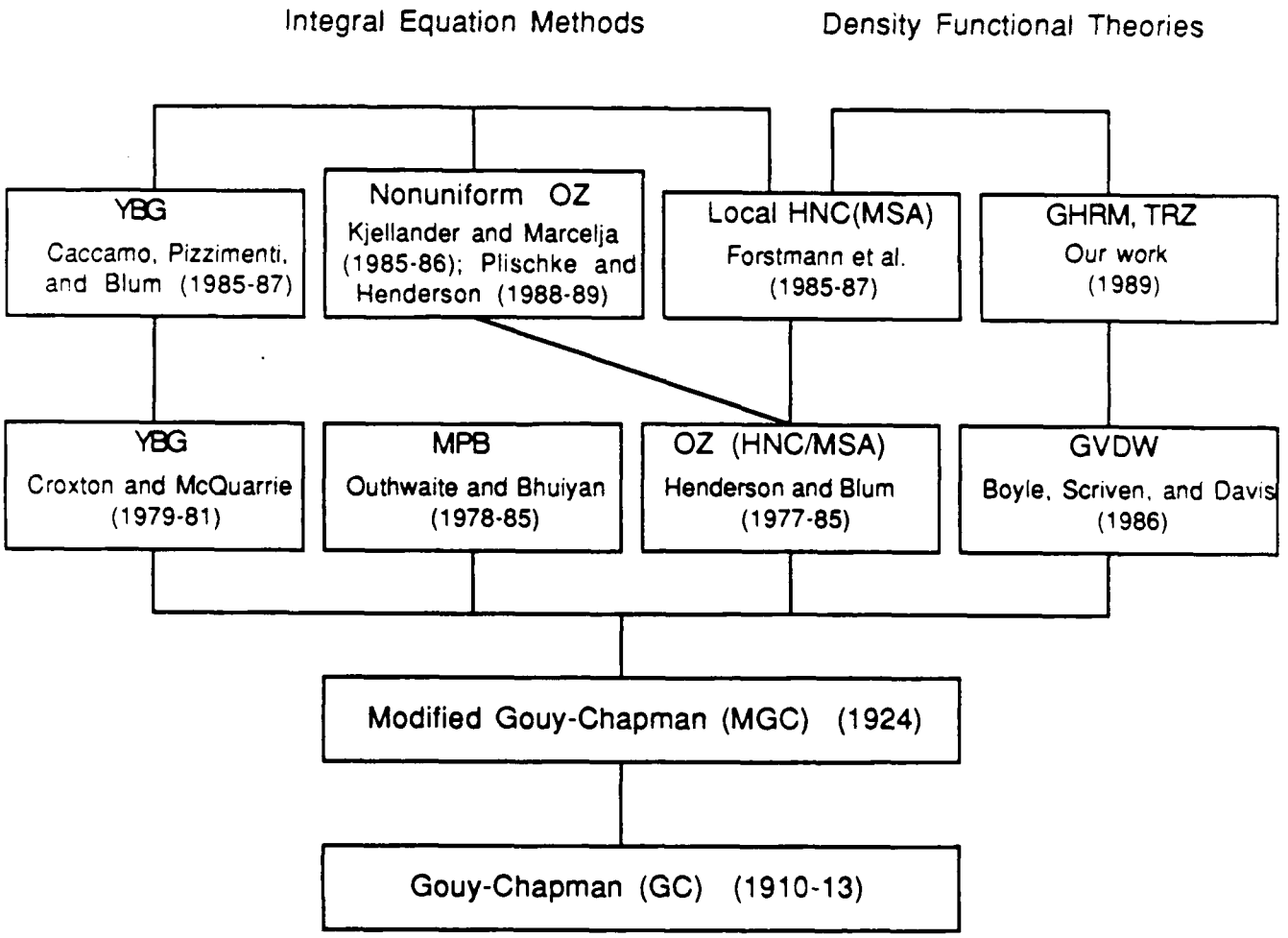

Table II. Diffuse layer potential $\Psi^*(0) = e\Psi(0)/kT$

c	σ^*	MC[a]	MGC	BGY[b]	$MPB5$[c]	PH[d]	$GHRM$[e]	$GVDW$[f]	TRZ[g]
				1:1 electrolytes					
0.01M	0.10	5.05(0.05)	5.44	—	5.08	4.58	5.26	5.242	5.243
0.1M	0.30	4.63(0.03)	5.34	5.00	4.74	4.37	4.76	4.49	4.54
1.0M	0.10	1.09(0.06)	1.40	1.055	1.03	1.06	1.03	1.00	1.01
	0.25	2.13(0.05)	2.79	2.31	2.10	2.22	2.18	2.01	2.05
	0.42	3.08(0.10)	3.74	3.46	3.02	3.23	3.23	2.68	2.88
	0.55	4.15(0.15)	4.26	4.21	—	4.22	4.12	3.12	3.61
	0.60	4.38(0.11)	4.43	4.48	—	4.68	4.52	3.29	3.96
	0.70	5.71(0.14)	4.74	5.02	—	5.76	5.41	3.69	4.79
2.0M	0.396	2.29(0.09)	2.99	2.303	—	2.29	2.19	1.68	1.88
				2:2 electrolytes					
0.05M	0.20	1.33(0.02)	2.61	1.81	1.36	1.18	1.59	1.539	1.543
0.5M	0.1704	0.63(0.04)	1.36	0.638	0.537	0.69	0.57	0.528	0.532

a. G. M. Torrie and J. P. Valleau, Ref. 4. Statistical uncertainty is shown in parenthesis.
b. C. Caccamo, G. Pizzimenti and L. Blum, Ref. 8; 1986.
c. C. W. Outhwaite and L. B. Bhuiyan, Ref. 7; 1986.
d. M. Plischke and D. Henderson, Ref. 10; 1988.
e. L. Mier-y-Teran, S. H. Suh, H. S. White, and H. T. Davis, Ref. 19.
f. This work. Results of the GVDW model.
g. This work. Results of the TRZ model.

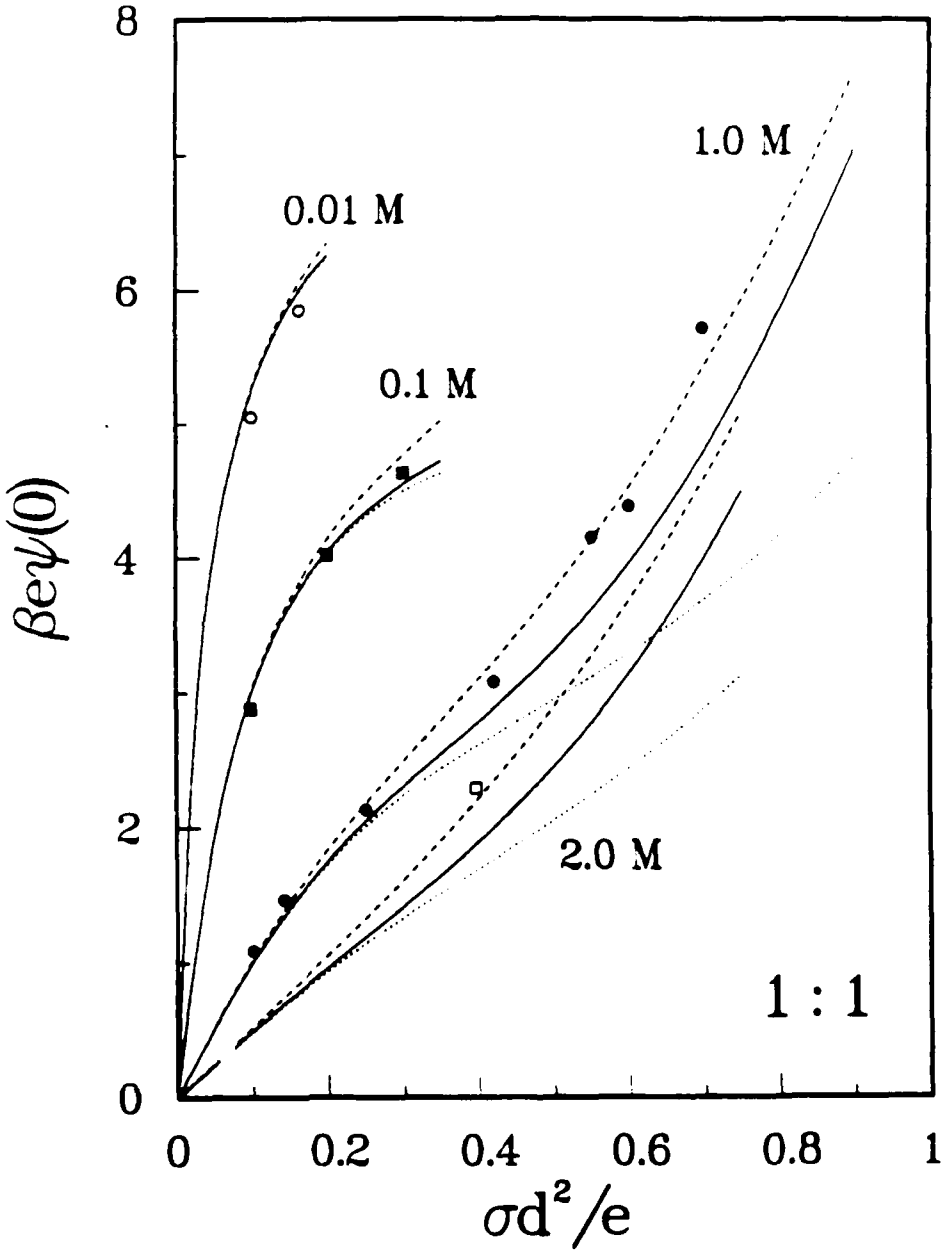

Figure 1

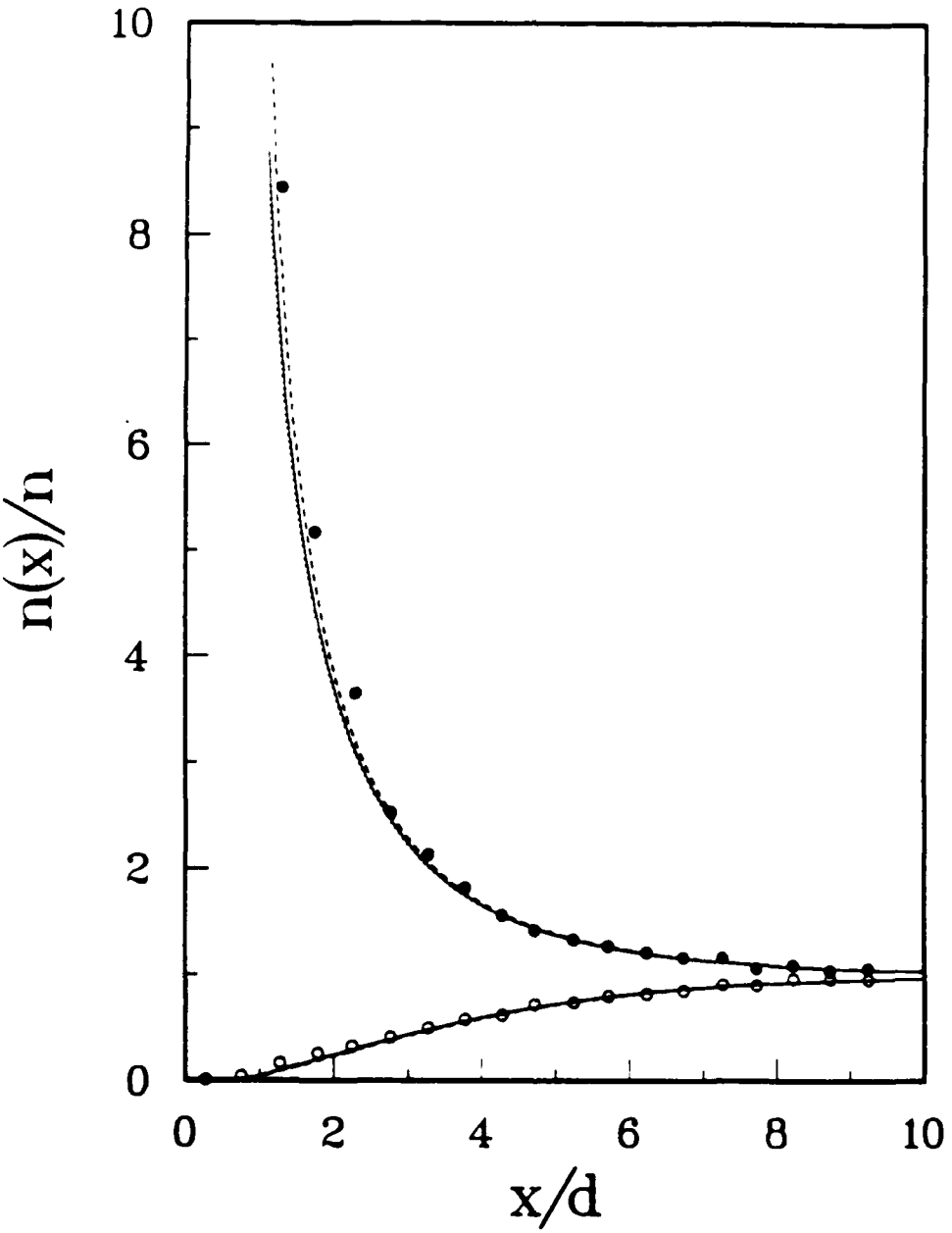

Figure 2

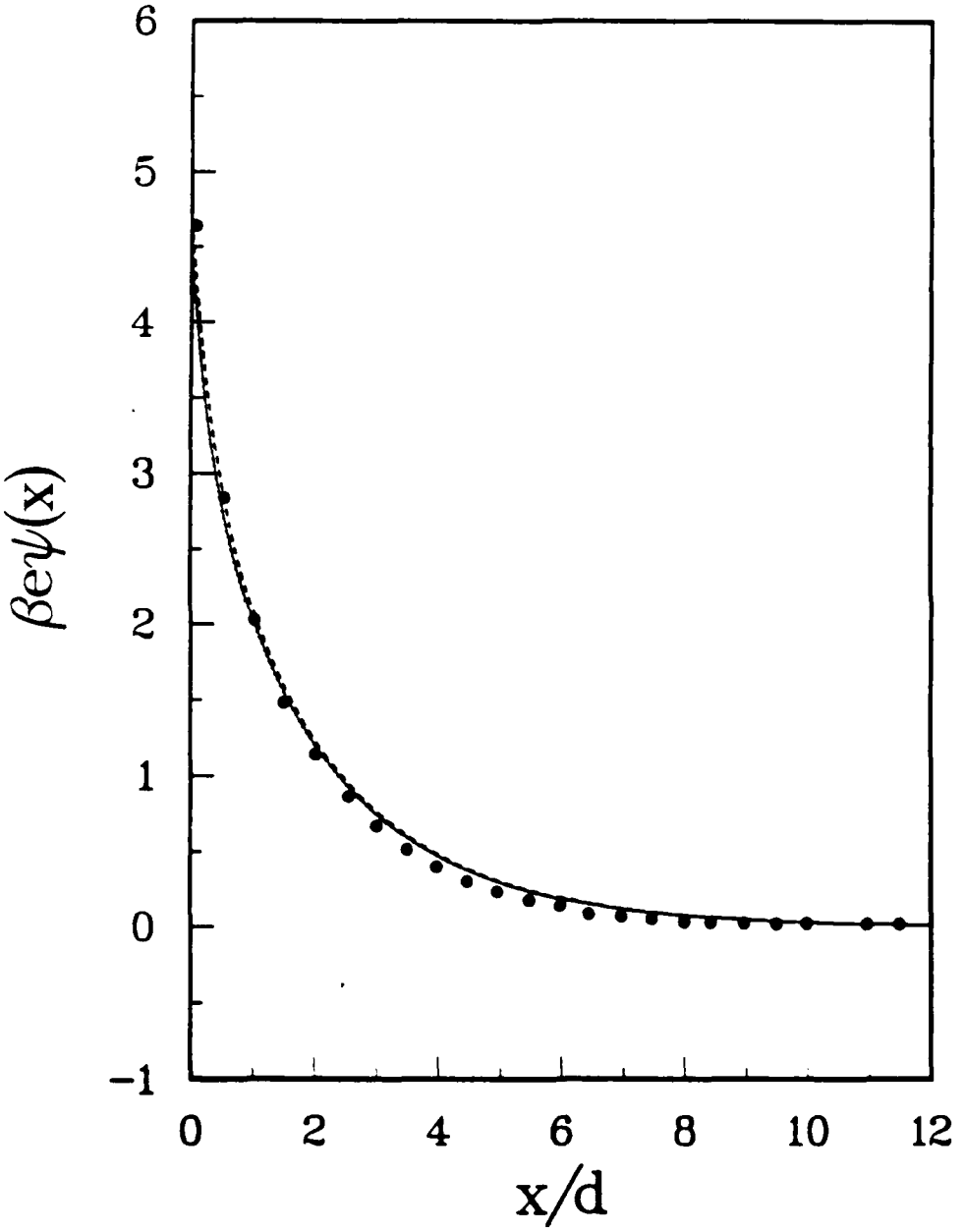

Figure 3

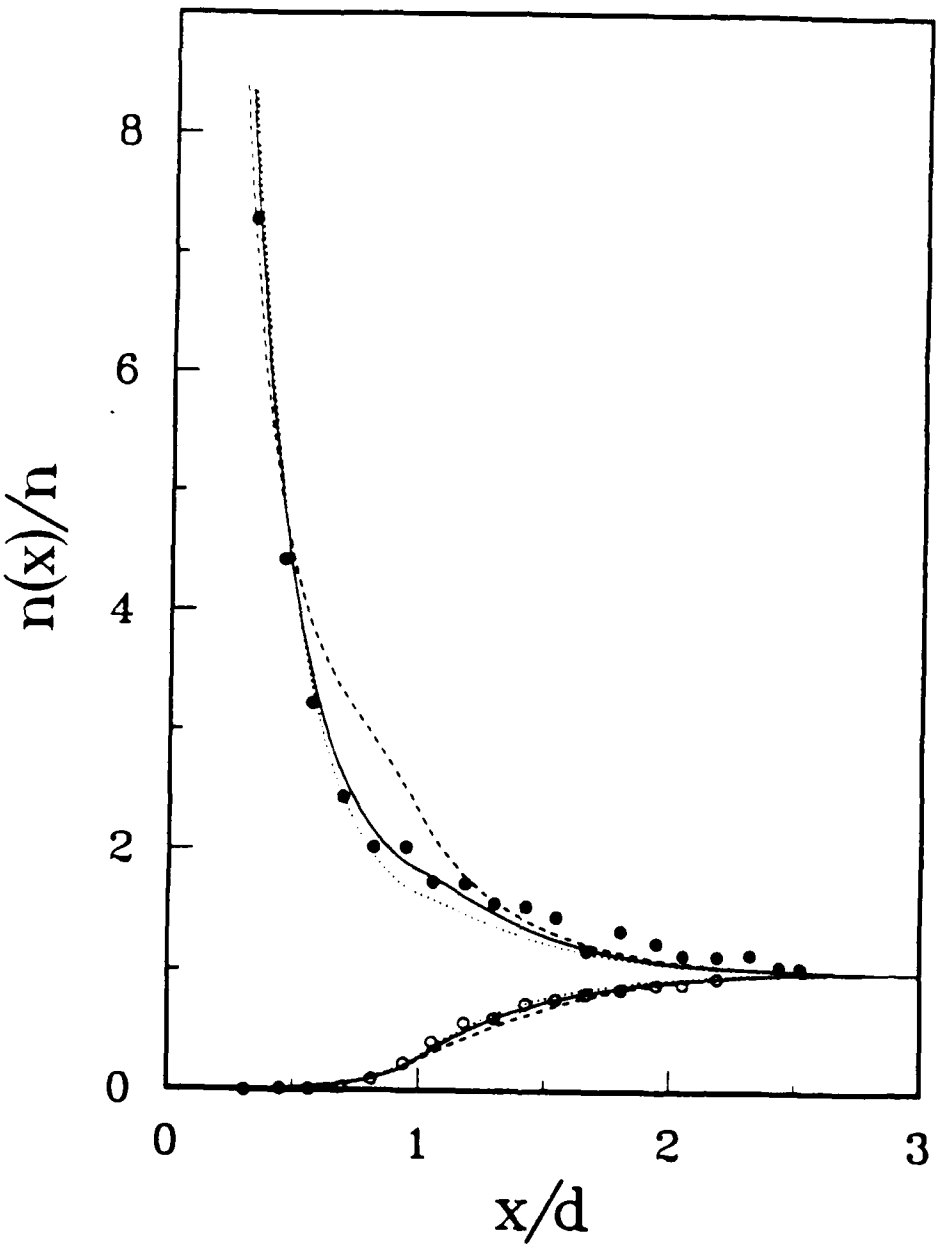

Figure 4

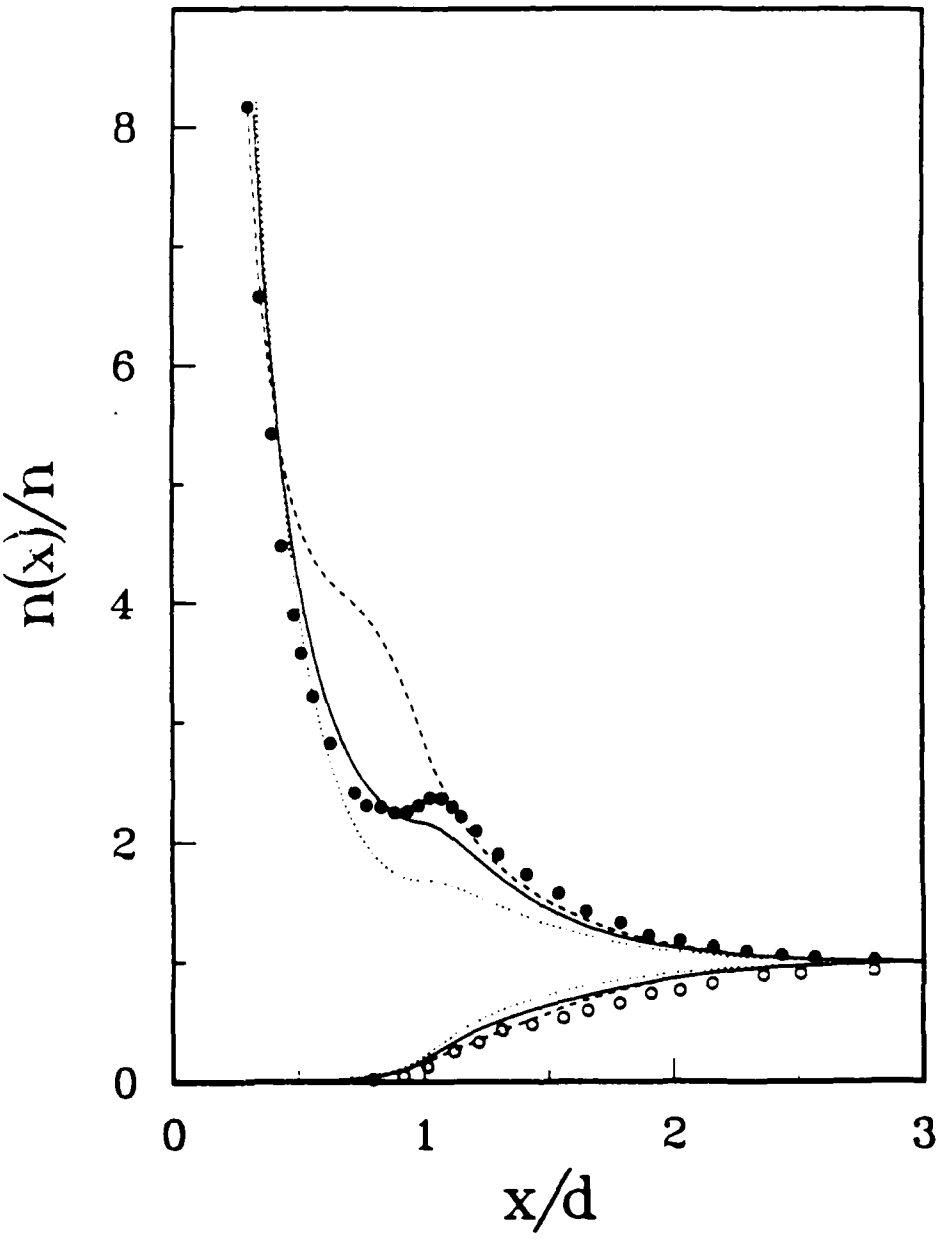

Figure 5

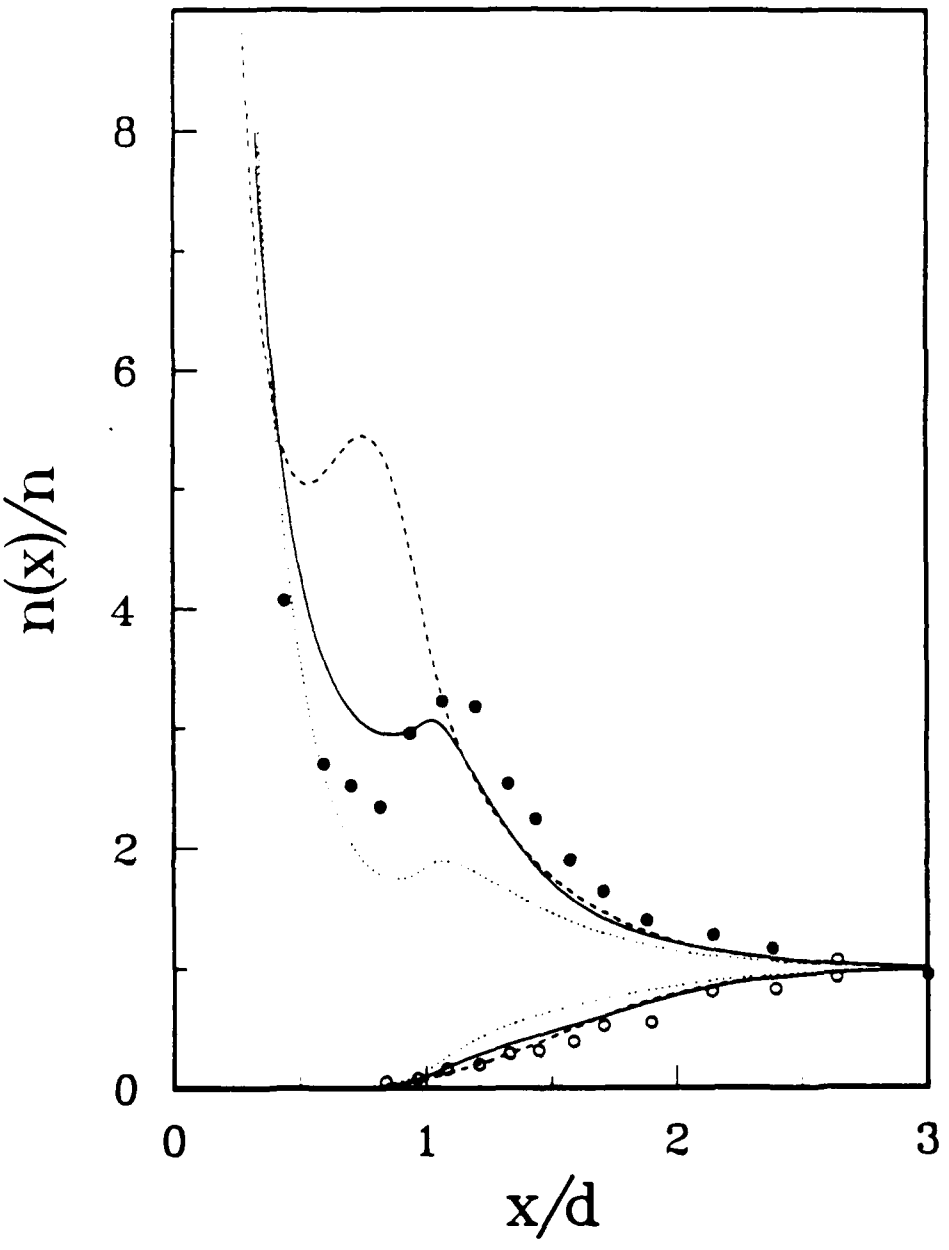

Figure 6

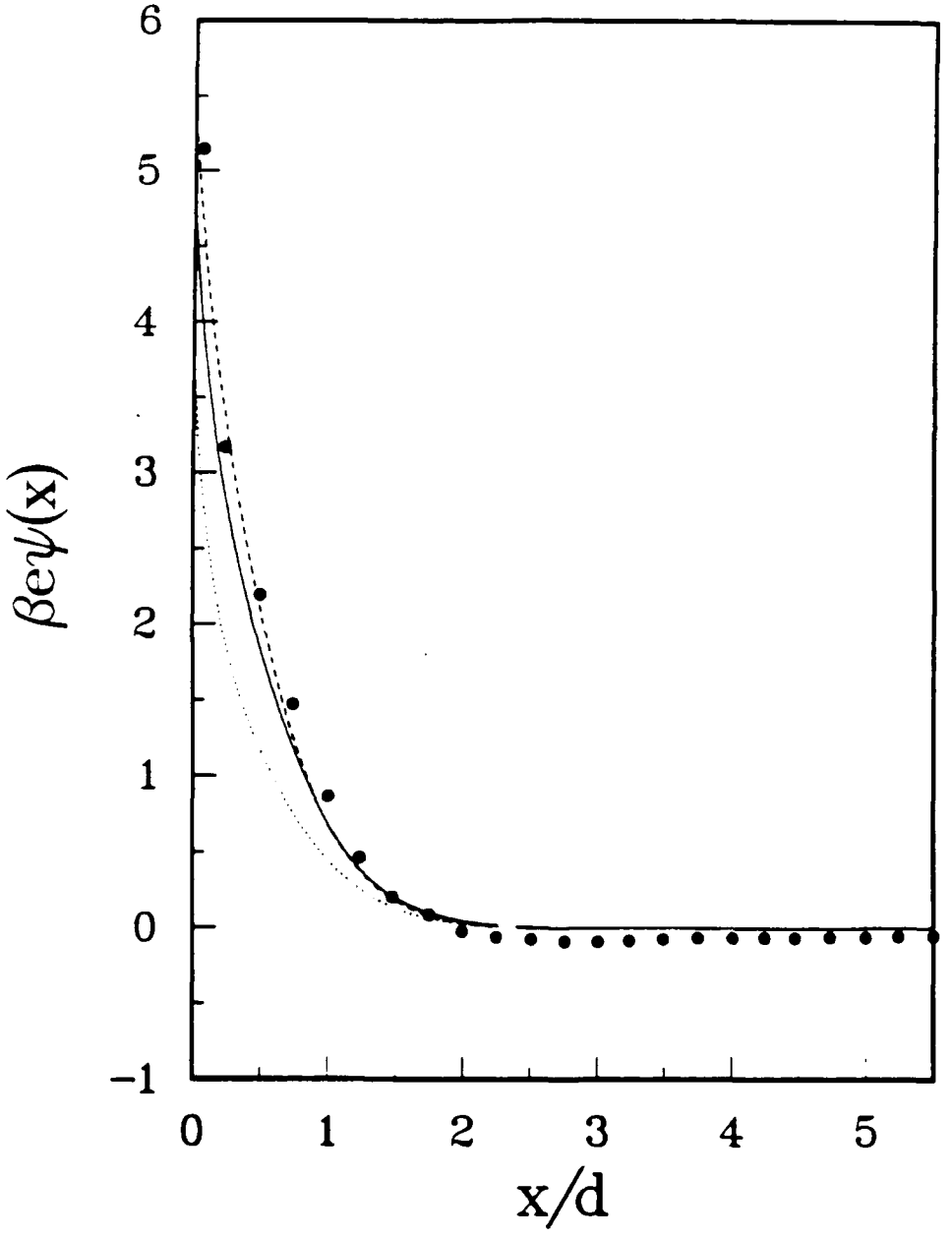

Figure 7

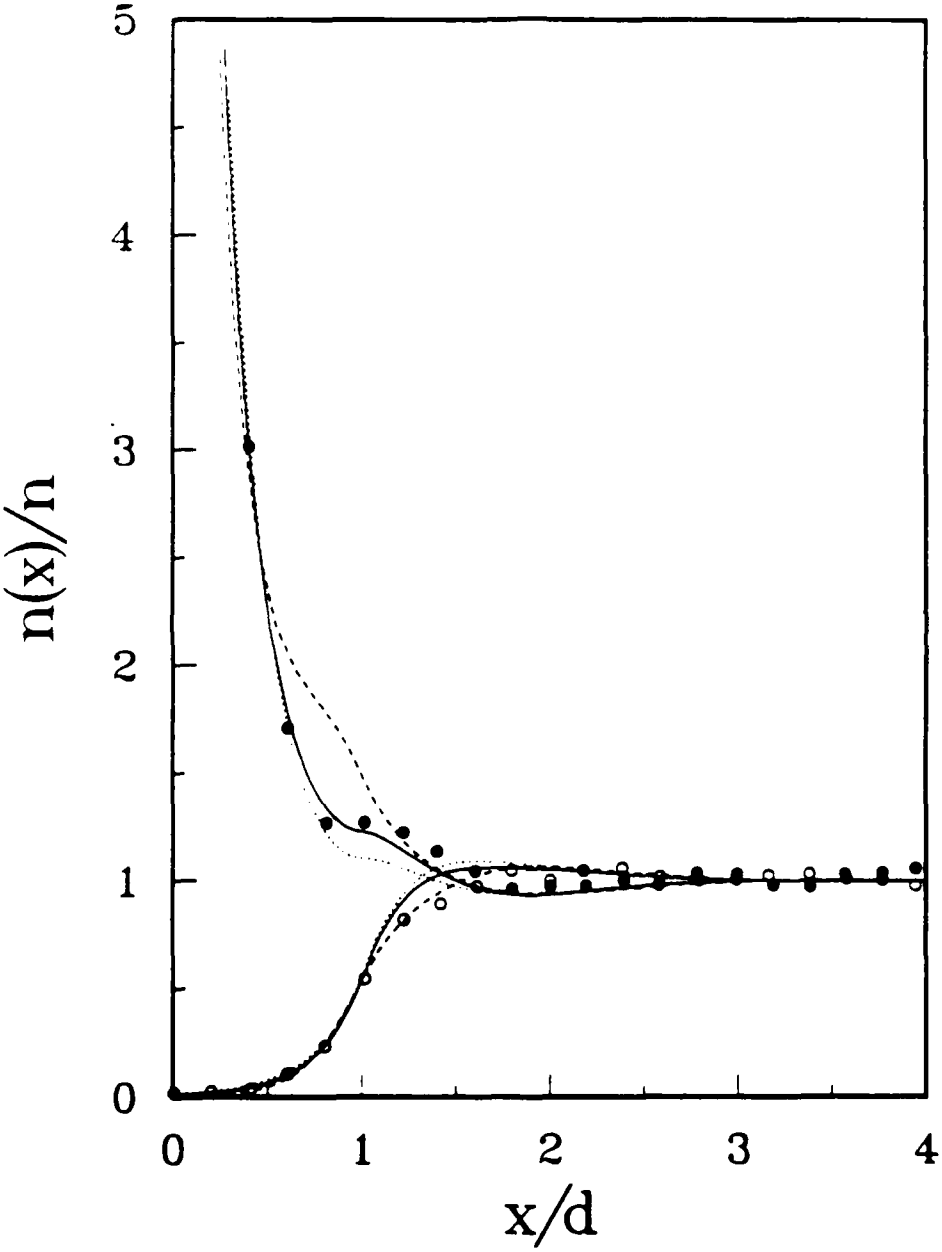

Figure 8

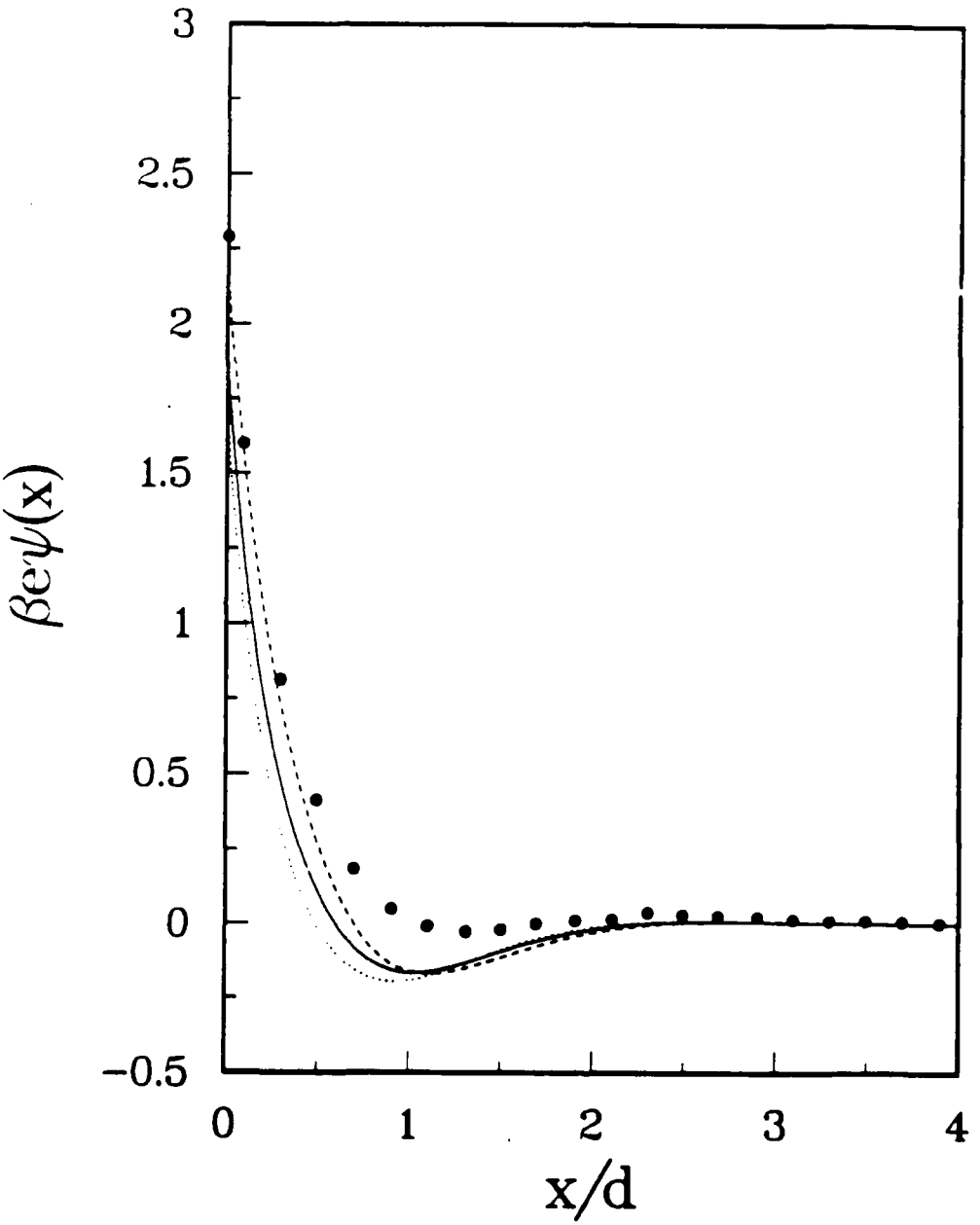

Figure 9

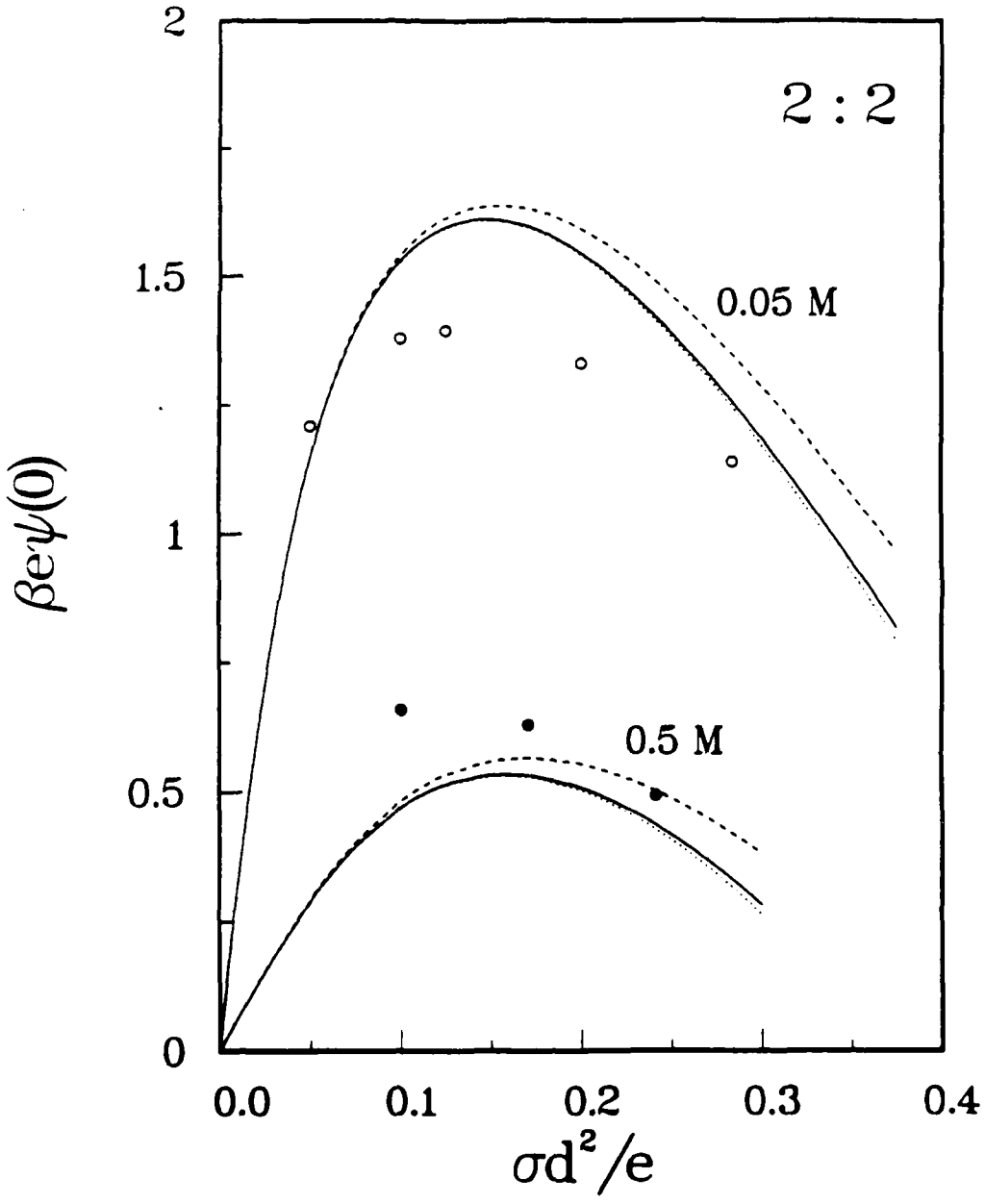

Figure 10

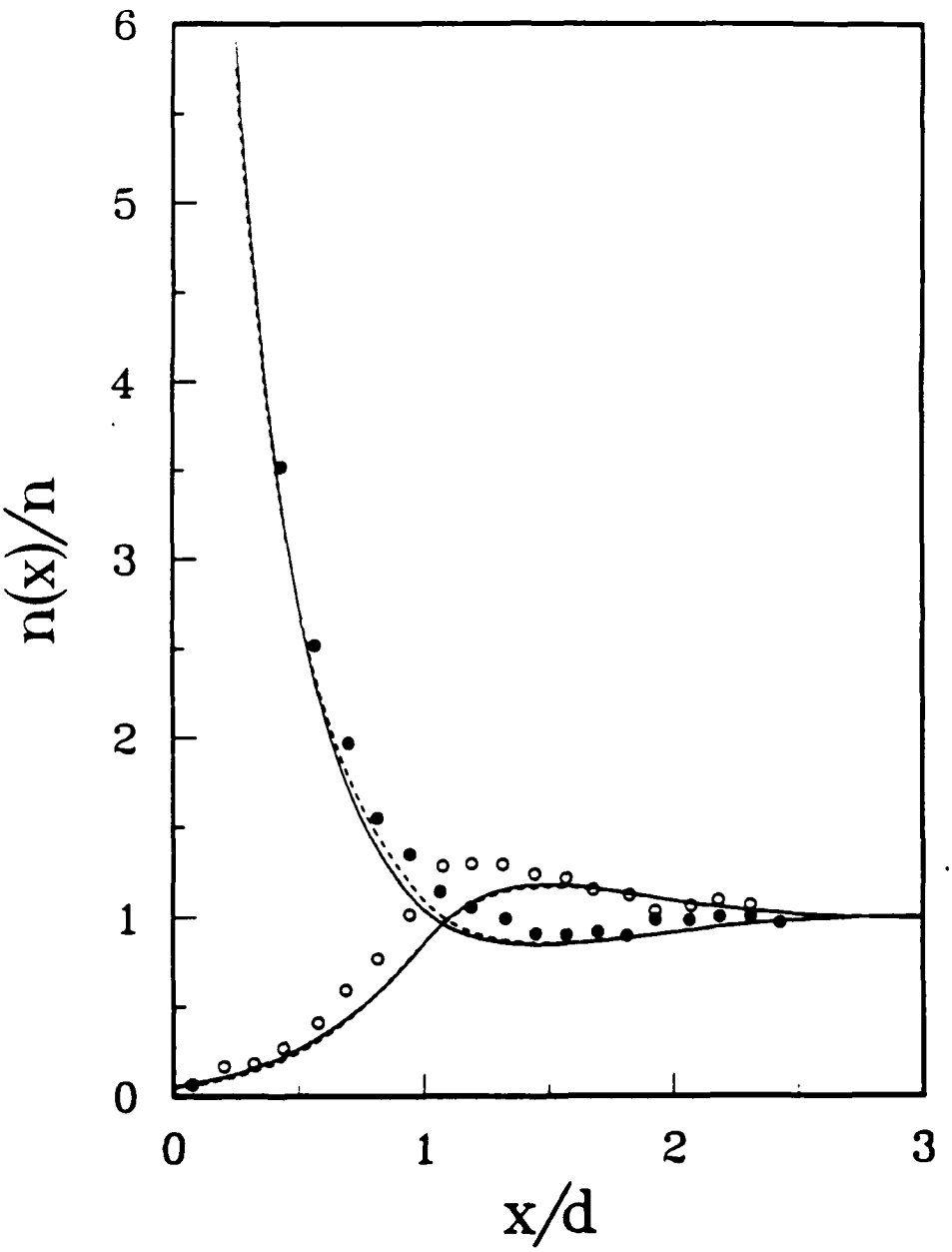

Figure 11

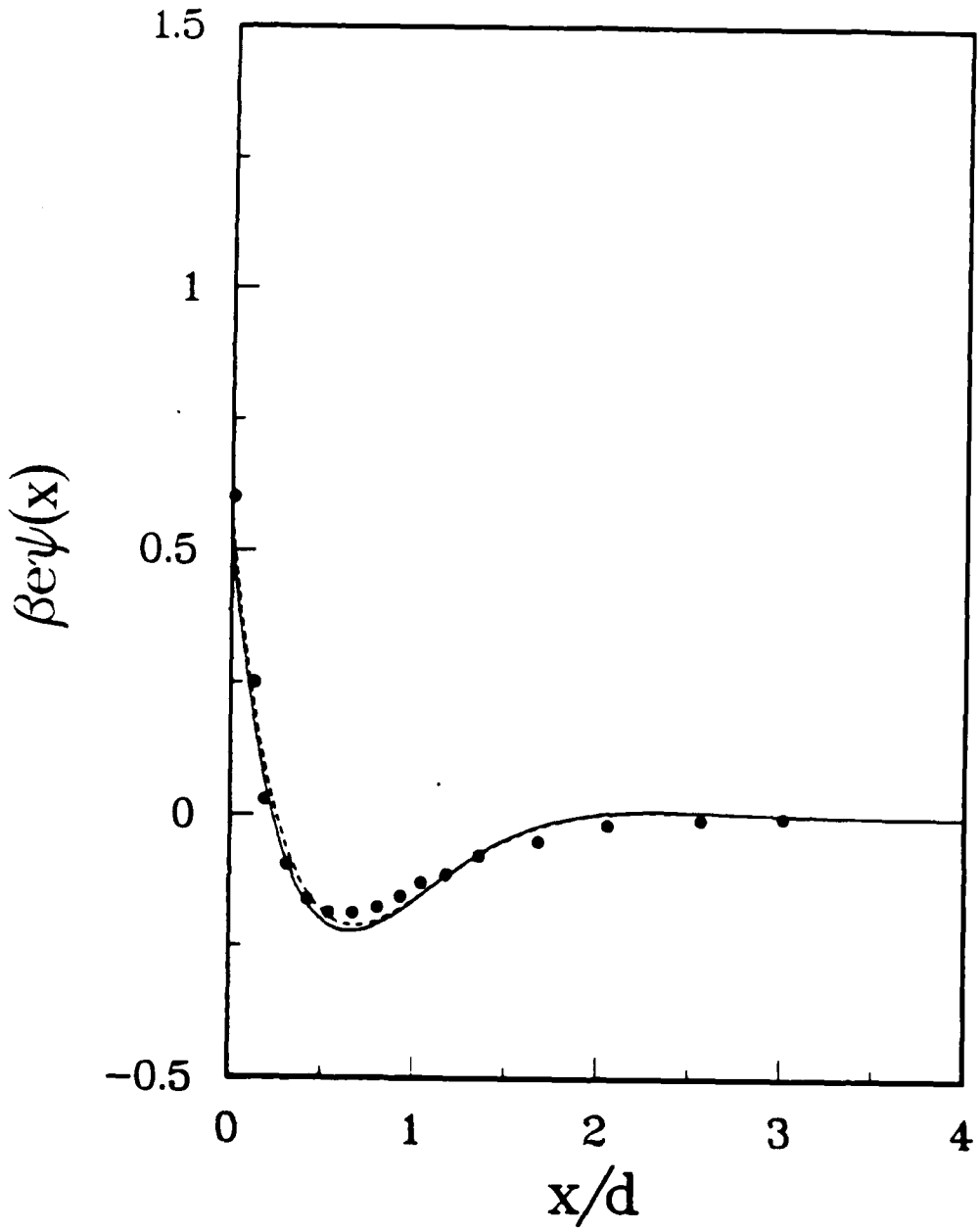

Figure 12